

LAW OFFICES  
MILLEN, WHITE, ZELANO & BRANIGAN, P.C.  
ARLINGTON COURTHOUSE PLAZA I  
SUITE 1400  
2200 CLARENDON BOULEVARD  
ARLINGTON, VIRGINIA 22201

TELEPHONE: (703) 243-6333  
CABLE: USALAW  
INT'L TELEX: 64191  
TELECOPIER: (703) 243-6410

Atty's Docket No. SCH-1733-P2

Applicant(s) : Dario NERI et al.

For : SPECIFIC BINDING MOLECULES FOR SCINTIGRAPHY, CONJUGATES CONTAINING THEM  
AND THERAPEUTIC METHOD FOR TREATMENT OF ANGIOGENESIS

THE COMMISSIONER OF PATENTS AND TRADEMARKS  
Washington, D.C. 20231

Sir:

Herewith is the above-identified application for Letters Patent including:

- ☒ Specification and claims (44 pages)
- ☒ Verified statement(s) to establish small entity status under 37 CFR 1.9 and 37 CFR 1.27
- ☒ 22 Sheets Drawings
- ☐ Formal ☐ Informal
- ☐ Information Disclosure
- ☒ Declaration and Power of Attorney
- ☐ Preliminary Amendment
- ☒ A check in the amount of \$ 771.00 (Check No. 15059) is attached.
- ☐ Please charge my Deposit Account No. 13-3402 in the amount of \$ \_\_\_\_\_.
- Two copies of this sheet are attached.

CLAIMS AS FILED					
	FOR	NUMBER FILED	NUMBER EXTRA	RATE	BASIC FEE \$
	TOTAL CLAIMS	35 -20=	15	x 18.00	270.00
	INDEPENDENT CLAIMS	5 - 3 =	2	x 78.00	156.00
	<input type="checkbox"/> Multiple Dependent Claim Presented				
			TOTAL FILING FEE		771.00

- ☐ The benefit under 35 U.S.C. §119 is claimed of the filing date of:
- ☐ A certified copy of the priority document(s) is attached.
- ☒ The Commissioner is hereby authorized to charge any deficiencies in payment of the following fees associated with this communication or credit any overpayment to Deposit Account No. 13-3402.
  - ☒ Any filing fees under 37 CFR 1.16 for the presentation of extra claims.
  - ☒ Any patent application processing fees under 37 CFR 1.17.
- ☒ The Commissioner is hereby authorized to charge payment of the following fees during the pendency of this application or credit any overpayments to Deposit Account No. 13-3402, two copies of this sheet are being enclosed.
  - ☒ Any patent application processing fees under 37 CFR 1.17.
  - ☒ The issue fee set in 37 CFR 1.18 at or before mailing of the Notice of Allowance, pursuant to 37 CFR 1.311(b).
  - ☒ Any filing fees under 37 CFR 1.16 for presentation of extra claims.

Respectfully submitted,

MILLEN, WHITE, ZELANO & BRANIGAN, P.C.

DATE: February 24, 2000

BY: Anthony J. Zelano (Reg. No. 27,969)

Serial or Patent No.: \_\_\_\_\_

Attorney's  
Locket No.: \_\_\_\_\_

1900 PTUS  
CP2

Filed or Issued: \_\_\_\_\_

For: SPECIFIC BINDING MOLECULES FOR SCINTIGRAPHY, CONJUGATES CONTAINING THEM

AND THERAPEUTICAL METHOD FOR TREATMENT OF ANGIOGENESIS

VERIFIED STATEMENT (DECLARATION) CLAIMING SMALL ENTITY STATUS

(37 CFR 1.9(f) and 1.27(c)) — SMALL BUSINESS CONCERN

I hereby declare that I am

- ( ) the owner of the small business concern identified below:  
(X) an official of the small business concern empowered to act on behalf of the concern identified below:

NAME OF CONCERN PHILOGEN S.r.l.

ADDRESS OF CONCERN Via Roma 22 - 53100 SIENA - ITALY

I hereby declare that the above identified small business concern qualifies as a small business concern as defined in 13 CFR 121.3-18, and reproduced in 37 CFR 1.9(d), for purposes of paying reduced fees under section 41(a) and (b) of Title 35, United States Code, in that the number of employees of the concern, including those of its affiliates, does not exceed 500 persons. For purposes of this statement, (1) the number of employees of the business concern is the average over the previous fiscal year of the concern of the persons employed on a full-time, part-time or temporary basis during each of the pay periods of the fiscal year, and (2) concerns are affiliates of each other when either, directly or indirectly, one concern controls or has the power to control the other, or a third party or parties controls or has the power to control both.

I hereby declare that rights under contract or law have been conveyed to and remain with the small business concern identified above with regard to the invention, entitled SPECIFIC BINDING MOLECULES FOR SCINTIGRAPHY, CONJUGATES CONTAINING THEM AND ...

Dario NERI, Lorenzo TARLI, Francesca VITI and Manfred BIRCHLER by inventor(s)

described in

- (X) the specification filed herewith  
( ) application serial no. \_\_\_\_\_, filed \_\_\_\_\_  
( ) patent no. \_\_\_\_\_, issued \_\_\_\_\_

If the rights held by the above identified small business concern are not exclusive, each individual, concern or organization having rights to the invention is listed below\* and no rights to the invention are held by any person, other than the inventor, who could not qualify as a small business concern under 37 CFR 1.9(d) or by any concern which would not qualify as a small business concern under 37 CFR 1.9(d) or a nonprofit organization under 37 CFR 1.9(e). \*NOTE: Separate verified statements are required from each person, concern or organization having rights to the invention averring to their status as small entities. (37 CFR 1.27)

NAME EIDGENÖSSISCHE TECHNISCHE HOCHSCHULE ZÜRICH

ADDRESS Rämistrasse 101 - CH-8092 ZÜRICH (Switzerland)

( ) INDIVIDUAL ( ) SMALL BUSINESS CONCERN (X) NONPROFIT ORGANIZATION

NAME \_\_\_\_\_

ADDRESS \_\_\_\_\_

( ) INDIVIDUAL ( ) SMALL BUSINESS CONCERN ( ) NONPROFIT ORGANIZATION

I acknowledge the duty to file, in this application or patent, notification of any change in status resulting in loss of entitlement to small entity status prior to paying, or at the time of paying, the earliest of the issue fee or any maintenance fee due after the date on which status as a small entity is no longer appropriate. (37 CFR 1.28(b))

I hereby declare that all statements made herein of my own knowledge are true and that all statements made on information and belief are believed to be true; and further that these statements were made with the knowledge that willful false statements and the like so made are punishable by fine or imprisonment, or both, under section 1001 of Title 18 of the United States Code, and that such willful false statements may jeopardize the validity of the application, any patent issuing thereon, or any patent to which this verified statement is directed.

NAME OF PERSON SIGNING Duccio NERI

TITLE OF PERSON OTHER THAN OWNER Sole Director

ADDRESS OF PERSON SIGNING Via delle Cantine 15 - 53100 SIENA - ITALY

SIGNATURE Duccio Neri DATE 4th February 2000

Applicant or Patentee Dario NERI, Lorenzo TARLI, Francesca VITI and Manfred BIRCHLER

Attorney's  
Docket No.:

Serial or Patent No. \_\_\_\_\_

Filed or Issued \_\_\_\_\_

For SPECIFIC BINDING MOLECULES FOR SCINTIGRAPHY, CONJUGATES CONTAINING THEM  
AND THERAPEUTICAL METHOD FOR TREATMENT OF ANGIOGENESIS  
VERIFIED STATEMENT (DECLARATION) CLAIMING SMALL ENTITY STATUS  
(37 CFR 1.9(f) and 1.27(d)) - NONPROFIT ORGANIZATION

I hereby declare that I am an official empowered to act on behalf of the nonprofit organization identified below:

NAME OF ORGANIZATION EIDGENÖSSISCHE TECHNISCHE HOCHSCHULE ZÜRICH

ADDRESS OF ORGANIZATION Rämistrasse 101 - CH-8092 ZÜRICH (Switzerland)

#### TYPE OF ORGANIZATION

(X) UNIVERSITY OR OTHER INSTITUTION OF HIGHER EDUCATION

( ) TAX EXEMPT UNDER INTERNAL REVENUE SERVICE CODE (26 USC 501(a) and 501(c)(3))

( ) NONPROFIT SCIENTIFIC OR EDUCATIONAL UNDER STATUTE OF STATE OF THE UNITED STATES OF AMERICA

(NAME OF STATE \_\_\_\_\_)

(CITATION OF STATUTE \_\_\_\_\_)

( ) WOULD QUALIFY AS TAX EXEMPT UNDER INTERNAL REVENUE SERVICE CODE (26 USC 501(a) and 501(c)(3)) IF LOCATED IN THE UNITED STATES OF AMERICA

( ) WOULD QUALIFY AS NONPROFIT SCIENTIFIC OR EDUCATIONAL UNDER STATUTE OF STATE OF THE UNITED STATES OF AMERICA IF LOCATED IN THE UNITED STATES OF AMERICA

(NAME OF STATE \_\_\_\_\_)

(CITATION OF STATUTE \_\_\_\_\_)

I hereby declare that the nonprofit organization identified above qualifies as a nonprofit organization as defined in 37 CFR 1.9(e) for purposes of paying reduced fees under section 41(a) or (b) of Title 35, United States Code with regard to the invention entitled SPECIFIC BINDING MOLECULES FOR SCINTIGRAPHY...  
by inventor(s) Dario NERI, Lorenzo TARLI, Francesca NERI and Manfred BIRCHLER  
described in

(X) the specification filed herewith

( ) application serial no. \_\_\_\_\_, filed \_\_\_\_\_

( ) patent no. \_\_\_\_\_, issued \_\_\_\_\_

I hereby declare that rights under contract or law have been conveyed to and remain with the nonprofit organization with regard to the above identified invention

If the rights held by the nonprofit organization are not exclusive, each individual, concern or organization having rights to the invention is listed below and no rights to the invention are held by any person, other than the inventor, who could not qualify as a small business concern under 37 CFR 1.9(d) or by any concern which would not qualify as a small business concern under 37 CFR 1.9(d) or a nonprofit organization under 37 CFR 1.9(e). NOTE: Separate verified statements are required from each named person, concern or organization having rights to the invention averring to their status as small entities. (37 CFR 1.27)

NAME PHILOGEN S.r.l.

ADDRESS Via Roma 22 - 53100 SIENA - ITALY

( ) INDIVIDUAL (X) SMALL BUSINESS CONCERN ( ) NONPROFIT ORGANIZATION

NAME \_\_\_\_\_

ADDRESS \_\_\_\_\_

( ) INDIVIDUAL ( ) SMALL BUSINESS CONCERN ( ) NONPROFIT ORGANIZATION

I acknowledge the duty to file, in this application or patent, notification of any change in status resulting in loss of entitlement to small entity status prior to paying, or at the time paying, the earliest of the issue fee or any maintenance fee due after the date on which status as a small entity is no longer appropriate. (37 CFR 1.28(b))

I hereby declare that all statements made herein of my own knowledge are true and that all statements made on information and belief are believed to be true; and further that these statements were made with the knowledge that willful false statements and the like so made are punishable by fine or imprisonment, or both, under section 1001 of Title 18 of the United States Code, and that such willful false statements may jeopardize the validity of the application, any patent issuing thereon, or any patent to which this verified statement is directed

NAME OF PERSON SIGNING Ulrich STEINER

TITLE IN ORGANIZATION EIDGENÖSSISCHE TECHNISCHE HOCHSCHULE ZÜRICH

ADDRESS OF PERSON SIGNING Rämistrasse 101, CH-8092 Zurich

Proctor for the  
Research and  
Industrial  
Liasons

SIGNATURE \_\_\_\_\_

Dr. U. Steiner  
ETH Transfer  
Rämistrasse 101  
CH 8092 Zürich

DATE 10.2.2000

03-02-00 15:46

## Field of the Invention

## Background of the Invention

Tumours cannot grow beyond a certain mass without the formation of new blood vessels (angiogenesis), and a correlation between microvessel density and tumour invasiveness has been reported for a number of tumours (Folkman (1995). *Nature Med.*, 1, 27-31). Moreover, angiogenesis underlies the majority of ocular disorders which result in loss of vision [Lee et al., *Surv. Ophthalmol.* 43, 245-269 (1998); Friedlander, M. et al., *Proc. Natl. Acad. Sci. U.S.A.* 93, 9764-9769 (1996)].

Molecules capable of selectively targeting markers of angiogenesis would create clinical opportunities for the diagnosis and therapy of tumours and other diseases characterised by vascular proliferation, such as diabetic retinopathy and age-related macular degeneration. Markers of angiogenesis are expressed in the majority of aggressive solid tumours and should be readily accessible to specific binders injected intravenously (Pasqualini et al. (1997). *Nature Biotechnol.*, 15, 542-546; Neri et al. (1997), *Nature Biotechnol.*, 15 1271-1275). Targeted occlusion of the neovasculature may result in tumour infarction and collapse (O'Reilly et al. (1996). *Nature Med.*, 2, 689-692; Huang et al. (1997). *Science*, 275, 547-550).

The ED-B domain of fibronectin, a sequence of 91 aminoacids identical in mouse, rat and human, which is inserted by alternative splicing into the fibronectin molecule, specifically accumulates around neo-vascular structures (Castellani et al. (1994). *Int. J. Cancer* 59, 612-618) and could represent a target for molecular

intervention. Indeed, we have recently shown with fluorescent techniques that anti-ED-B single-chain Fv antibody fragments (scFv) accumulate selectively in tumoural blood vessels of tumour-bearing mice, and that antibody affinity appears to dictate targeting performance (Neri et al. (1997). *Nature Biotechnol.*, 15 1271-1275; International Patent Application No. PCT/GB97/01412, based on GB96/10967.3). Tumour targeting was evaluated 24 hours after injection, or at later time points.

Various attempts are known in the art to raise antibodies against the ED-B-domain in order to use them for tumour targeting.

- 10 Peters et al. (*Cell Adhesion and Communication* 1995, 3: 67-89) disclose polyclonal antibodies raised to antigens containing no FN sequence other than the intact ED-B domain and show that they bind specifically and directly to this domain.

- 15 However, the reagents of Peters et al. suffer from a series of drawbacks:- the antisera of Peters et al. recognise ED-B(+)-FN only after treatment with N-glycanase. This makes these reagents unsuitable for applications such as tumour targeting, imaging and therapy, as deglycosylation cannot be performed in vivo.

- The authors acknowledge themselves that their antibodies do not recognise full-length ED-B(+)-FN produced by mammalian cells. They also acknowledge that it  
20 had been impossible to produce monoclonal antibodies specific for the ED-B domain of fibronectin, even though antibodies against other domains of fibronectin (such as ED-A) had been produced. It is well-known in the art that polyclonal antisera are unacceptable for above mentioned applications.

- Even after years of intense research in this field, monoclonal antibodies  
25 recognising the ED-B domain of fibronectin without treatment with N-glycanase could be produced only using phage display techniques as applied in the present invention.

- Zang et al. (*Matrix Biology* 1994, 14: 623-633) disclose a polyclonal antiserum raised against the canine ED-B domain. The authors do expect a cross-reactivity  
30 to human ED-B(+)-FN, although this was not tested. However, the authors acknowledge the difficulty to produce monoclonal antibodies directly recognising the ED-B domain of fibronectin (page 631). The antiserum recognises ED-B(+)-FN

in Western blot only after treatment with N-glycanase. As mentioned before, glycanase treatment renders these reagents unsuitable for applications according to the present invention.

Recognition of ED-B(+)-FN in ELISA proceeds without the need of deglycosylation but only on cartilage extracted with a denaturing agent (4M Urea) and captured on plastic using gelatin. The authors comment that "the binding of the FN molecule to the gelatine bound on the plastic surface of the ELISA plate may somehow expose the epitopes sufficiently for recognition by the antiserum". Since for *in vivo* applications FN cannot be denatured and gelatin bound, the monoclonal binders of the present invention offer distinct advantages.

The Japanese patents JP02076598 and JP04169195 refer to anti-ED-B antibodies. It is not clear from these documents if monoclonal anti ED-B antibodies are described. Moreover, it seems impossible that a single antibody (such as the antibody described in JP02076598) has "an antigen determinant in aminoacid sequence of formulae (1), (2) or (3):

- (1) EGIPIFEDFVDSSVG Y
- (2) YTVTGLEPGIDYDIS
- (3) NGGESAPTTLTQQ T

on the basis of the following evidence:

- i) A monoclonal antibody should recognise a well-defined epitope.
- ii) The three-dimensional structure of the ED-B domain of fibronectin has been determined by NMR spectroscopy. Segments (1), (2) and (3) lie on opposite faces of the ED-B structure, and cannot be bound simultaneously by one monoclonal antibody.

Furthermore, in order to demonstrate the usefulness of the antibodies localisation in tumours should be demonstrated, as well as evidence of staining of ED-B(+)-FN structures in biological samples without treatment with structure-disrupting reagents.

The BC1 antibody described by Carnemolla et al. 1992, J. Biol. Chem. 267, 24689-24692, recognises an epitope on domain 7 of FN, but not on the ED-B domain, which is cryptic in the presence of the ED-B domain of fibronectin. It is strictly human-specific. Therefore, the BC1 antibody and the antibodies of the

present invention show different reactivity. Furthermore, the BC1 antibody recognises domain 7 alone, and domain 7-8 of fibronectin in the absence of the ED-B domain (Carnemolla et al. 1992, J. Biol. Chem. 267, 24689-24692). Such epitopes could be produced in vivo by proteolytic degradation of FN molecules.

5 The advantage of the reagents according to the present invention is that they can localise on FN molecules or fragments only if they contain the ED-B domain.

For the diagnosis of cancer, and more specifically for imaging primary and secondary tumour lesions, immunoscintigraphy is one of the techniques of choice. In this methodology, patients are imaged with a suitable device (e.g., a gamma  
10 camera), after having been injected with radiolabelled compound (e.g., a radionuclide linked to a suitable vehicle). For scintigraphic applications, short-lived gamma emitters such as technetium-99m, iodine-123 or indium-111 are typically used, in order to minimise exposure of the patient to ionising radiations.

The most frequently used radionuclide in Nuclear Medicine Departments is  
15 technetium-99m (99mTc), a gamma emitter with half-life of six hours. Patients injected with 99mTc-based radiopharmaceuticals can typically be imaged up to 12-24 hours after injections; however, accumulation of the nuclide on the lesion of interest at earlier time points is desirable.

Furthermore, if antibodies capable of rapid and selective localisation on newly-  
20 formed blood vessels were available, researchers would be stimulated to search for other suitable molecules to conjugate to antibodies, in order to achieve diagnostic and/or therapeutic benefit.

#### Summary of the Invention

Considering the need of nuclear medicine for radiopharmaceuticals capable of  
25 localising tumour lesions few hours after injection, and the information that antibody affinity appears to influence its performance in targeting of angiogenesis, it is an object of the present invention to produce antibodies specific for the ED-B domain of fibronectin with sub-nanomolar dissociation constant (for a review on the definitions and measurements of antibody-antigen affinity, see Neri et al.  
30 (1996). Trends in Biotechnol. 14, 465-470). A further object of the present invention is to provide radiolabelled antibodies in suitable format, directed against the ED-B domain of fibronectin, that detect tumour lesions already few hours after

In one aspect of the invention these objects are achieved by an antibody with specific affinity for a characteristic epitope of the ED-B domain of fibronectin and with improved affinity to said ED-B epitope.

Another aspect of the present invention is a diagnostic kit comprising said antibody and one or more reagents for detecting angiogenesis.

Finally, an important aspect of the invention is represented by conjugates comprising said antibodies and a suitable photoactive molecules (e.g. a judiciously chosen photosensitizer), and their use for the selective light-mediated occlusion of new blood vessels.

Throughout the application several technical expressions are used for which the following definitions apply.

20 This describes an immunoglobulin whether natural or partly or wholly synthetically produced. The term also covers any polypeptide or protein having a binding domain which is, or is homologous to, an antibody binding domain. These can be derived from natural sources, or they may be partly or wholly synthetically produced. Examples of antibodies are the immunoglobulin isotypes and their  
25 isotypic subclasses; fragments which comprise an antigen binding domain such as Fab, scFv, Fv, dAb, Fd; and diabodies. It is possible to take monoclonal and other antibodies and use techniques of recombinant DNA technology to produce other antibodies or chimeric molecules which retain the specificity of the original antibody. Such techniques may involve introducing DNA encoding the  
30 immunoglobulin variable region, or the complementarity determining regions (CDRs), of an antibody to the constant regions, or constant regions plus framework regions, of a different immunoglobulin. See, for instance, EP-A-184187,



GB 2188638A or EP-A-239400. A hybridoma or other cell producing an antibody may be subject to genetic mutation or other changes, which may or may not alter the binding specificity of antibodies produced. As antibodies can be modified in a number of ways, the term "antibody" should be construed as covering any specific binding member or substance having a binding domain with the required specificity. Thus, this term covers antibody fragments, derivatives, functional equivalents and homologues of antibodies, including any polypeptide comprising an immunoglobulin binding domain, whether natural or wholly or partially synthetic. Chimeric molecules comprising an immunoglobulin binding domain, or equivalent, fused to another polypeptide are therefore included. Cloning and expression of chimeric antibodies are described in EP-A-0120694 and EP-A-0125023. It has been shown that fragments of a whole antibody can perform the function of binding antigens. Examples of binding fragments are (i) the Fab fragment consisting of VL, VH, CL and CH1 domains; (ii) the Fd fragment consisting of the VH and CH1 domains; (iii) the Fv fragment consisting of the VL and VH domains of a single antibody; (iv) the dAb fragment (Ward et al. (1989) *Nature*, ), 341, 544-546.) which consists of a VH domain; (v) isolated CDR regions; (vi) F(ab')<sub>2</sub> fragments, a bivalent fragment comprising two linked Fab fragments; (vii) single chain Fv molecules (scFv), wherein a VH domain and a VL domain are linked by a polypeptide linker which allows the two domains to associate to form an antigen binding site (Bird et al. (1988) *Science*, 242, 423-426.; Huston et al. (1988) *Proc. Natl. Acad. Sci. U.S.A.*, 85, 5879-83.); (viii) bispecific single chain FV dimers (PCT/US92/09965) and (ix) "diabodies", multivalent or multispecific fragments constructed by gene fusion (WO94/13804; Holliger et al. (1993) *Proc. Natl. Acad. Sci. U.S.A.*, 90, 6444-6448). Diabodies are multimers of polypeptides, each polypeptide comprising a first domain comprising a binding region of an immunoglobulin light chain and a second domain comprising a binding region of an immunoglobulin heavy chain, the two domains being linked (e.g. by a peptide linker) but unable to associate with each other to form an antigen binding site: antigen binding sites are formed by the association of the first domain of one polypeptide within the multimer with the second domain of another polypeptide within the multimer (WO94/13804). Where bispecific antibodies are to be used,

these may be conventional bispecific antibodies, which can be manufactured in a variety of ways Holliger and Winter (1993), *Curr. Opin. Biotech.*, 4, 446-449), e.g. prepared chemically or from hybrid hybridomas, or may be any of the bispecific antibody fragments mentioned above. It may be preferable to use scFv dimers or

5 diabodies rather than whole antibodies. Diabodies and scFv can be constructed without an Fc region, using only variable domains, potentially reducing the effects of anti-idiotypic reaction. Other forms of bispecific antibodies include the single-chain CRAbs described by Neri et al. ((1995) *J. Mol. Biol.*, 246, 367-373).

- complementarity-determining regions

- 10 Traditionally, complementarity-determining regions (CDRs) of antibody variable domains have been identified as those hypervariable antibody sequences, containing residues essential for specific antigen recognition. In this document, we refer to the CDR definition and numbering of Chothia and Lesk (1987) *J. Mol. Biol.*, 196, 901-917.

- 15 - functionally equivalent variant form

This refers to a molecule (the variant) which although having structural differences to another molecule (the parent) retains some significant homology and also at least some of the biological function of the parent molecule, e.g. the ability to bind a particular antigen or epitope. Variants may be in the form of fragments,

20 derivatives or mutants. A variant, derivative or mutant may be obtained by modification of the parent molecule by the addition, deletion, substitution or insertion of one or more aminoacids, or by the linkage of another molecule. These changes may be made at the nucleotide or protein level. For example, the encoded polypeptide may be a Fab fragment which is then linked to an Fc tail from

25 another source. Alternatively, a marker such as an enzyme, fluorescein, etc, may be linked. For example, a functionally equivalent variant form of an antibody "A" against a characteristic epitope of the ED-B domain of fibronectin could be an antibody "B" with different sequence of the complementarity determining regions, but recognising the same epitope of antibody "A".

- 30 We have isolated recombinant antibodies in scFv format from an antibody phage display library, specific for the ED-B domain of fibronectin, and recognising ED-B(+)-fibronectin in tissue sections. One of these antibodies, E1, has been affinity

matured to produce antibodies H10 and L19, with improved affinity. Antibody L19 has a dissociation constant for the ED-B domain of fibronectin in the sub-nanomolar concentration range.

The high-affinity antibody L19 and D1.3 (an antibody specific for an irrelevant antigen, hen egg lysozyme) were radiolabelled and injected in tumour-bearing mice. Tumour, blood and organ biodistributions were obtained at different time points, and expressed as percent of the injected dose per gram of tissue (%ID/g). Already 3 hours after injection, the %ID/g (tumour) was better than the %ID/g (blood) for L19, but not for the negative control D1.3. The tumour : blood ratios increased at longer time points. This suggests that the high-affinity antibody L19 may be a useful tumour targeting agent, for example for immunoscintigraphic detection of angiogenesis.

- photosensitizer (or photosensitiser)

A photosensitiser could be defined as a molecule which, upon irradiation and in the presence of water and/or oxygen, will generate toxic molecular species (e.g., singlet oxygen) capable of reacting with biomolecules, therefore potentially causing damage to biological targets such as cells, tissues and body fluids.

Photosensitisers are particularly useful when they absorb at wavelengths above 600 nm. In fact, light penetration in tissues and body fluids is maximal in the 600 – 900 nm range [Wan et al. (1981) *Photochem. Photobiol.* **34**, 679-681].

The targeted delivery of photosensitisers followed by irradiation is an attractive avenue for the therapy of angiogenesis-related diseases [Yarmush, M.L. *et al.* Antibody targeted photolysis. *Crit. Rev. Therap. Drug Carrier Systems* **10**, 197-252 (1993); Rowe, P.M. *Lancet* **351**, 1496 (1998); Levy, J. *Trends Biotechnol.* **13**, 14-18 (1995)), particularly for the selective ablation of ocular neovasculation. Available therapeutic modalities such as laser photocoagulation, either directly or after administration of photosensitising agents, are limited by a lack of selectivity and typically result in the damage of healthy tissues and vessels [Macular Photocoagulation Study Group, *Arch. Ophthalmol.* **112**, 480-488 (1994); Haimovici, R. *et al.*, *Curr. Eye Res.* **16**, 83-90 (1997); Schmidt-Erfurth, U. *et al.*; *Graefes Arch. Clin. Exp. Ophthalmol.* **236**, 365-374 (1998)].

On the basis of the arguments presented above, one can see that it would be

extremely important to discover ways to improve the selectivity and specificity of photosensitisers, for example by conjugating them to a suitable carrier molecule. It is likely that the development of good-quality carrier molecules will not be a trivial task. Moreover, it is likely that not all photosensitisers will lend themselves to be  
 5 „vehicled« in vivo to the site of interest. Factors such as photosensitiser chemical structure, solubility, lipophilicity, stickiness and potency are likely to crucially influence the „targetability« and efficacy of photosensitisers' conjugates.

Here we show that the high-affinity L19 antibody, specific for the ED-B domain of fibronectin, selectively localises to newly formed blood vessels in a rabbit model of  
 10 ocular angiogenesis upon systemic administration. The L19 antibody, chemically coupled to the photosensitising agent tin (IV) chlorin  $e_6$  and irradiated with red light, mediated the selective occlusion of ocular neovasculature and promoted apoptosis of the corresponding endothelial cells. These results demonstrate that new ocular blood vessels can be distinguished immunochemically from pre-  
 15 existing ones in vivo, and strongly suggest that targeted delivery of photosensitisers followed by irradiation may be effective in treating blinding eye diseases and possibly other pathologies associated with angiogenesis.

Another important feature to be considered when conjugates containing a photosensitisers are used is the fact that photosensitisers are among the few  
 20 species capable of mediating their toxic activity in the immediate proximity of the antibody to which they have been conjugated.

Upon irradiation and in the presence of oxygen, most photosensitisers produce, among other reactive species, singlet oxygen: a diffusive toxic molecule capable of damaging cells by reacting with membranes, proteins and DNA. The average  
 25 diffusion of singlet oxygen has been estimated to be around 200 nm (Yarmush et al. 1993, Crit. Rev. Ther. Drug, 10, 197-252).

The same applies to alpha-emitting radionuclides, such as astatine-211, bismuth-212 and bismuth-213, which produce energetic alpha particles having a range in tissue penetration of 50-100  $\mu\text{M}$  (Hauck et al. 1998, Brit. J. Cancer 77, 753-759),  
 30 depositing energy that is about 500 times greater than that of beta particles, e.g. yttrium-90 (100 KeV/ $\mu\text{M}$  vs. 0.2 KeV/ $\mu\text{M}$ , respectively) (McDevitt et al. 1998, Eur. J. Nucl. Med. 25, 1341-135).

Photosensitisers or alpha-emitting radionuclides conjugated to the antibodies specific for the ED-B domain of fibronectin described in the present application, as for example L 19, can be targeted to new blood vessels in vivo, as illustrated in the examples hereinafter reported. Thanks to this exquisite specificity of localisation and to the short range of action of the toxic species released by photosensitiser

and alpha-emitting radionuclides, specific damage can be inferred in the immediate proximity of the labelled antibody, while sparing adjacent tissues/cells. Toxic species with a short path of action (such as singlet oxygen and alpha particles), when delivered by the L19 antibody, offer the possibility to selectively damage the endothelial cells of new blood vessels, while sparing normal tissues and blood cells. This level of selectivity should offer tremendous advantages for the control of angiogenesis-related disorders, such as cancer, rheumatoid arthritis, neo-vasculature associated ocular disorders and psoriasis.

The innovative concept of delivering short-range acting toxic agents to new blood vessels, while sparing established blood vessels and normal tissues, can be easily appreciated in the light of the following considerations.

Let us consider the biodistribution studies performed in tumour-bearing mice injected with radiolabelled L19, described in Example 3. When using the L19 antibody labelled with a beta-particle emitting radionuclide (e.g., Yttrium-90), the antibody delivers beta particles to the neighbouring cells/tissues with a penetration of several millimetres. Let us assume that all tissues in the body are equally radiosensitive, let us neglect radioactive decay, and let us remember that radioactivity will begin to exhibit its biocidal effect from the moment the radiolabelled antibody is injected intravenously (i.e., from time = 0 s). The therapeutic advantage of the radiolabelled antibody will be related to the ratio between the total dose of radioactivity delivered by the antibody to the tumour and the total dose of radioactivity delivered by the antibody to blood or organs, normalised per gram of fluid or tissue (Behr et al. 1998, *Int. J. Cancer* 77, 787-795).

Let us examine the biocidal dose delivered to the tumour and to blood (representative of myelotoxicity, which is typically the limiting toxicity with radiolabelled antibodies).

The dose of radioactivity delivered per gram of tumour is proportional to the area under the curve (AUC) of the %ID/g (tumour), plotted versus time. Analogously, the dose of radioactivity delivered to blood is proportional to the area under the curve (AUC) of the %ID/g (blood), plotted versus time. During the first 24 hours  
 5 after intravenous injection the ratio of  $AUC(\text{tumour}) / AUC(\text{blood})$  is equal to 3.6 (Figure 13). This ratio may somewhat increase when the AUCs are measured for longer time periods, but therapeutic ratios greater than 6-7 are rarely achieved.

Let us now consider the situation in which a short-range-acting toxic species (e.g., a photosensitiser or an alpha-particle emitting radionuclide) is delivered to the  
 10 tumoural blood vessels, and is therefore not homogeneously distributed in the tumour mass. The diffusive toxic species (e.g., singlet oxygen or an alpha particle) will hardly penetrate more than one layer of cells, i.e. will hit only the endothelial cells lining the tumour blood vessel wall. Since new-forming blood vessels in most tumours (including the F9 teratocarcinoma) constitute less than 2% of the total  
 15 tumour mass, the relevant parameter for predicting therapeutic benefit will be the ratio  $AUC(\text{vessel}) / AUC(\text{blood})$ .

As we can see in Figure 14, L19 accumulates only around new blood vessels. This observation has also been confirmed by microautoradiographic analysis in tumours (Tarli et al. 1999, Blood, 94, 192-198). Since the radioactivity delivered to  
 20 tumours is concentrated around neo-vascular structures, and assuming that tumoural vasculature accounts for 2% of the tumour weight, we can calculate that  $AUC(\text{vessel}) = (100/2) \times AUC(\text{tumour}) = 50 \times AUC(\text{tumour})$ . In other words, the selectivity of the treatment is expected to be proportional to the ratio  $AUC(\text{vessel}) / AUC(\text{blood})$ , which is  $> 150:1$  over a period of 24 hours in our experimental  
 25 system (see also Figure 15 for explanation).

Let us consider astatine-211 as a particularly interesting alpha-particle emitting radionuclide for biomedical application. The half-life of its radioactive decay is considerably longer than the ones of bismuth-212 and bismuth-213 (7.2 hrs, compared to 1.0 hr and 45 min., respectively) (Larsen and Bruland 1998, Brit. J.  
 30 Cancer 77, 1115-1122). Astatine is the heaviest halogen and no stable isotopes of this element exist. Since it is directly below iodine in the periodic table, it might be expected that the two halogens would possess similar chemical properties.

However, attempts to label proteins with  $^{211}\text{At}$  by direct electrophilic astatination at the level of the protein amino acid did not give successful results because of rapid loss of label following *in vivo* administration (Vaughan et al. 1978, Int. J. Nucl. Med. 5, 229-230). To circumvent this problem, L19 can be conjugated with  $^{211}\text{At}$  with significant nuclide incorporation and no loss of antibody specificity by the two-step labeling method published by Garg (Garg et al. 1989, Appl. Radiat. Isot. 40, 485-490). It involves the use of a bifunctional chemical compound, N-succinimidyl-3-(trimethylstannyl)-benzoate (m-MeATE; ATE, «alkyltin ester») (Zalutsky et al. 1989, Proc. Natl. Acad. Sci. USA 86, 7149-7153), which we synthesized following the protocol published by Garg (see Figure 16) as reported in Example 7.

It is important to report that using equimolar amount of m-bromobenzoic acid and trimethylstannyl-chloride, the reaction product is 3-(trimethylstannyl)benzoic acid rather than the published trimethylstannyl-3-(trimethylstannyl) benzoate. Based on the results of the labeling experiments, described below, we believe that this compound may have superior qualities compared to the previously described trimethylstannyl-3-(trimethylstannyl) benzoate derivatives.

The bifunctional m-MeATE agent can be used both to label L19 with the gamma-emitting iodine-125 and the alpha-emitting astatine-211 in a two-step methodology. Protein labeling with iodine-125 through m-MeATE rather than conventional electrophilic methods (e.g, the chloramine-T and the Iodogen methods) is reported to provide protein iodination sites which are more inert towards dehalogenation *in vivo* (Garg et al. 1989, Appl. Radiat. Isot. 40, 485-490). The labeling protein coupling efficiency together with the conjugate immunoreactivity arising from this two-step radiolabeling methodology were studied through the reaction with iodine-125.

In the first step, m-MeATE and t-buthylhydroperoxide (TBHP) were added to  $\text{Na}^{125}\text{I}$ . Following a 20 minutes incubation period, the radioiodinated product N-succinimidyl-3-( $^{125}\text{I}$ )-benzoate was isolated and separated from unconjugated m-MeATE by chromatography using a disposable silica gel Sep-Pak column and a gradient of ethyl acetate in hexane as eluent phase. Starting from 100  $\mu\text{Ci}$  of  $\text{Na}^{125}\text{I}$ , we coupled 90  $\mu\text{Ci}$  of  $^{125}\text{I}$  to the N-succinimidyl benzoate. A solution of L19 in borate buffer (pH = 8.5) was added in the second step to the purified N-

succinimidyl-3-( $^{125}\text{I}$ )-benzoate. Following an incubation time of 30 minutes on ice, the radiolabelled L19 was separated from unincorporated iodine using a PD-10 disposable gel filtration column. The resulting efficiency of L19 labeling using radioiodinated ATE resulted to be strongly dependent on initial protein concentration. Using L19 at a concentration of 0.42  $\mu\text{g}/\mu\text{l}$  and 1  $\mu\text{g}/\mu\text{l}$ , 18% and 28% of starting radiolabelled benzoate was coupled to L19, respectively. According to these results, if we started from 1 mCi of  $\text{Na}^{125}\text{I}$  and a concentration of L19 of 1  $\mu\text{g}/\mu\text{l}$ , we would obtain L19 labelled with  $^{125}\text{I}$  at a specific activity of 1  $\mu\text{Ci}/\mu\text{l}$ . The initial concentration of L19 did not influence the immunoreactivity of the conjugates after labeling. Following the method reported in example 3, the immunoreactivity, defined as reported by Viti et al. (Viti et al. 1999, Cancer Research 59, 347-352) resulted to be in both cases > 90%.

These results demonstrate the feasibility of the labeling of L19 with radiohalogens using the bifunctional m-MeATE.

Astatine-211 may offer the additional advantage that it is likely to be detached from L19 by dehalogenases in the kidney glomeruli (T. M. Behr et al. 1999, Cancer Res. 59, 2635-43), but not in tumoural vessels, therefore reducing kidney toxicity of the radiolabelled compound in spite of the clearance of the immunoconjugate via the renal route. For photosensitisers, glomeruli in the kidneys will not be damaged, since for most applications irradiation of the kidneys is not foreseen.

It is obviously also possible to prepare conjugates consisting of the antibody linked to a photosensitiser and a radionuclide in order to take advantages of the activity of both.

#### Brief Description of the Drawings

Embodiments of the present invention are illustrated by the following figures, wherein

Fig. 1 shows a designed antibody phage library;

Fig. 2 shows 2D gels and Western blotting of a lysate of human melanoma COLO-38 cells;

Fig. 3 shows immunohistochemical experiments of glioblastoma multiforme

Fig. 4 shows an analysis of the stability of antibody-(ED-B) complexes.

Fig. 5 shows biodistribution of tumour bearing mice injected with radiolabelled



antibody fragments.

Fig. 6 shows amino acid sequence of L19;

Figure 7 shows rabbit eyes with implanted pellet;

Figure 8 shows immunohistochemistry of rabbit cornea sections.

- 5 Figure 9 shows the immunohistochemistry of sections of ocular structures of rabbits (cornea, iris and conjunctiva) using a red alkaline phosphatase substrate and hematoxylin.

Figure 10 shows the localisation of fluorescently-labelled antibodies in ocular neovasculature.

- 10 Figure 11 shows the macroscopic appearance of the eyes of rabbits injected with proteins coupled to photosensitizers, before and after irradiation.

Figure 12 shows the microscopic analysis of sections of ocular structures of rabbits injected with proteins coupled to photosensitizers and irradiated with red light.

- 15 Figure 13 shows schematic diagrams in which the % of injected dose delivered per gram, respectively of blood and tumour, are plotted versus time.

Figure 14 shows the accumulation of L19 around new vessels.

Figure 15 shows schematic diagrams reporting the relevant % of injected doses per gram, in the case of the L19 antibody coupled to an  $\alpha$ - and  $\beta$ -emitter respectively, plotted versus time.

- 20 Figure 16 shows the labelling method according to the Garg protocol modified as described hereinafter.

Figures 17a and 17b report the  $^1\text{H}$ -NMR spectrum of 3-(trimethylstannyl)-benzoic acid.

- 25 Figures 18 a and 18b report the  $^1\text{H}$ -NMR spectrum of N-succinimidyl-3-(trimethylstannyl)-benzoate

Figure 19 shows the EI-MS of N-succinimidyl-3-(trimethylstannyl)-benzoate.

#### Detailed Description of the Drawings

Figure 1 shows:

- 30 Designed antibody phage library. (a) Antibody fragments are displayed on phage as pIII fusion, as schematically depicted. In the antibody binding site (antigen's eye view), the  $\text{V}_\text{K}$  CDRs backbone is in yellow, the  $\text{V}_\text{H}$  CDR backbone is in blue.

Residues subject to random mutation are Vk CDR3 positions 91, 93, 94 and 96 (yellow), and VH CDR3 positions 95, 96, 97, and 98 (blue). The Cb atoms of these side chains are shown in darker colours. Also shown (in grey), are the residues of CDR1 and CDR2, which can be mutated to improve antibody affinity. Using the program RasMol (<http://www.chemistry.ucsc.edu/wipke/teaching/rasmol.html>), the structure of the scFv were modeled from pdb file 1igm (Brookhaven Protein Data Bank; <http://www2.ebi.ac.uk/pcserv/pdbdb.htm>). (b) PCR amplification and library cloning strategy. The DP47 and DPK22 germline templates were modified (see text) to generate mutations in the CDR3 regions. Genes are indicated as rectangles, and CDRs as numbered boxes within the rectangle. The VH and the VL segments were then assembled and cloned in pDN332 phagemid vector. Primers used in the amplification and assembly are listed at the bottom.

Figure 2 shows

2D gels and western blotting (a) Silver-staining of the 2D-PAGE of a lysate of human melanoma COLO-38 cells, to which recombinant ED-B-containing 7B89 had been added. The two 7B89 spots (circle) are due to partial proteolysis of the His-tag used for protein purification. (b) Immunoblot of a gel, identical to the one of Fig. 2a, using the anti-ED-B E1 (Table 1) and the M2 anti-FLAG antibodies as detecting reagent. Only the 7B89 spots are detected, confirming the specificity of the recombinant antibody isolated from a gel spot.

Figure 3 shows:

Immunohistochemical experiments on serial sections of glioblastoma multiforme showing the typical glomerulus-like vascular structures stained using scFvs E1 (A), A2 (B) and G4 (C). Scale bars: 20  $\mu$ m.

Figure 4 shows:

Stability of antibody-(ED-B) complexes. Analysis of the binding of scFvs E1, H10 and L19 to the ED-B domain of fibronectin. (a) BIAcore sensograms, showing the improved dissociation profiles obtained upon antibody affinity-maturation. (b) Native gel electrophoretic analysis of scFv-(ED-B) complexes. Only the high-affinity antibody L19 can form a stable complex with the fluorescently labelled antigen. Fluorescence detection was performed as described (Neri et al. (1996) *BioTechniques*, 20, 708-712).

(c) Competition of the scFv-(ED-B-biotin) complex with a 100-fold molar excess of unbiotinylated ED-B, monitored by electrochemiluminescence using an Origen apparatus. A long half-life for the L19-(ED-B) complex can be observed. Black squares: L19; Open triangles: H10.

5 Figure 5 shows:

Biodistributions of tumour bearing mice injected with radiolabelled antibody fragments.

Tumour and blood biodistributions, expressed as percent injected dose per gram, are plotted versus time. Relevant organ biodistributions is also reported.

10 Figure 6 shows the amino acid sequence of antibody L19 comprising the heavy chain (VH), the linker and the light chain (VL).

Figure 7 shows rabbit eyes with implanted polymer pellets soaked with angiogenic substances.

Figure 8 shows immunohistochemistry of sections of rabbit cornea with new-  
15 forming blood vessels, stained with the L19 antibody.

Figure 9 shows immunohistochemical studies of ocular structures using the L19 antibody. A specific red staining is observed around neovascular structures in the cornea (a), but not around blood vessels in the iris (b) and in the conjunctiva (c). Small arrows: corneal epithelium. Relevant blood vessels are indicated with large  
20 arrows. Scale bars: 50  $\mu$ m

Figure 10 shows immunophotodetection of fluorescently labelled antibodies targeting ocular angiogenesis. A strongly fluorescent corneal neovascularisation (indicated by an arrow) is observed in rabbits injected with the antibody conjugate L19-Cy5 (a), specific for the ED-B domain of FN, but not with the antibody HyHEL-  
25 10-Cy5 (b). Immunofluorescence microscopy on cornea sections confirmed that L19-Cy5 (c), but not HyHEL-10-Cy5 (d) localises around neovascular structures in the cornea. Images (a,b) were acquired 8 h after antibody injection; (c, d) were obtained using cornea sections isolated from rabbits 24 h after antibody injection. P, pellet.

30 Figure 11 shows macroscopic images of eyes of rabbits treated with photosensitiser conjugates. Eye of rabbit injected with L19-PS before (a) and 16 h after irradiation with red light (b). The arrow indicates coagulated neovasculature,

which is confirmed as a hypofluorescent area in the Cy5 fluoroangiogram of panel (c) 16 h after irradiation. Note that no coagulation is observed in other vascular structures, for example in the dilated conjunctival vessels. For comparison, a Cy5 fluoroangiogram with hyperfluorescence of leaky vessels, and the corresponding colour photograph of untreated rabbit eye are shown in (d) and (h). Pictures (e,f,g) are analogous to (a,b,c), but correspond to a rabbit injected with ovalbumin-PS and irradiated with red light. No coagulation can be observed, and the angiogram reveals hyperfluorescence of leaky vessels. The eyes of rabbits with early-stage angiogenesis and injected with L19-PS are shown in (i-l). Images before (i) and 16 h after irradiation with red light (j) reveal extensive and selective light-induced intravascular coagulation (arrow). Vessel occlusion (arrow) is particularly evident in the irradiated eye (l) of a rabbit immediately after euthanasia, but cannot be detected in the non-irradiated eye (k) of the same rabbit. P, pellet. Arrowheads indicate the corneo-scleral junction (limbus). In all figures, dilated pre-existing conjunctival vessels are visible above the limbus, whereas growth of corneal neovascularisation can be observed from the limbus towards the pellet (P).

Figure 12 shows microscopic analysis of selective blood vessel occlusion. H/E sections of corneas (a,e,b,f: non-fixed; i,j: paraformaldehyde fixed) of rabbits injected with ovalbumin-PS (a,e,i) or L19-PS (b,f,j) and irradiated. Large arrows indicate representative non damaged (e,i) or completely occluded (f,j) blood vessels. In contrast to the selective occlusion of corneal neovasculature and restricted perivascular damage (eosinophilia) mediated by L19-PS after irradiation (b,f,j), vessels in the conjunctiva (k) and iris (l) do not show sign of damage in the same rabbit. Fluorescent TUNEL assay indicates the different number of apoptotic cells in sections of irradiated rabbits injected with L19-PS (c,g) or with ovalbumin-PS (d,h). Large arrows indicate some relevant vascular structures. Small arrows indicate corneal epithelium. Scale bars: 100  $\mu\text{m}$  (a-d) and 25  $\mu\text{m}$  (e-l)

Figure 13 shows the area under the curve (AUC) of the radioactivity delivered by scFv(L19) to the blood and to the tumour during the first 24 hours after intravenous injection. In this experimental study performed in mice bearing the F9 teratocarcinoma, the AUC of the injected dose of radiolabelled antibody delivered

per gram of tumour is 3.6-fold higher than the dose delivered per gram of blood. This ratio increases when the AUC is measured for longer time periods.

Figure 14 shows microautoradiographic analysis of an F9 teratocarcinoma dissected from a nude mouse, after injection of radiolabelled scFv(L19). The pictures show that scFv(L19) accumulates around vascular structure but not in the surrounding normal mouse tissue.

Figure 15 illustrates a schematic diagram of the radiommunotherapy performed with the anti-angiogenesis scFv(L19) coupled with  $\beta$ - or  $\alpha$ -emitting radionuclide.

Because new-forming blood vessels in F9 teratocarcinoma constitute 0.5-5% of the total tumour mass, the radioactivity delivered to vascular structures is significantly higher (70-700-fold) than the one delivered to normal tissue and to blood. Coupling scFv(L19) to a beta emitter (e.g., Yttrium-90), the majority of the targeted tumoural area is irradiated, since these  $\beta$ -particles have a range in tissue of several millimeters. On the other hand, coupling scFv(L19) to an alpha emitter (e.g. Astatine-211 or Bismuth-212 or Bismuth-213), the radiation is deposited only around the targeted tumoural blood vessels (penetration: few dozens of micrometers). In this case, the relevant parameters for therapeutic efficacy is the vessel: blood ratio of the percent injected dose of radioactivity per gram of tissue, rather than the tumour: blood ratio (which is the relevant parameter for beta emitting nuclides).

Figure 16 shows the procedure for labelling scFv(L19) with Iodine-125 and Astatine-211 using the N-succinimidyl 3-(trimethylstannyl)benzoate (m-MeATE) synthesized from m-bromobenzoic acid.

Figure 17A shows the  $^1\text{H}$ -NMR spectrum of 3-(trimethylstannyl)benzoic acid in  $\text{CDCl}_3$ . The chemical shifts (ppm) are indicated in the X-axis.

Figure 17B shows the chemical shift in ppm of the protons in the aromatic moiety located at low magnetic field of the NMR spectrum.

Figure 18A shows the  $^1\text{H}$ -NMR spectrum of m-MeATE in  $\text{CDCl}_3$ . The relative values of peak intensity are reported between the X-axis reporting the chemical shift (ppm) and the spectrum baseline.

Figure 18B shows an enlarged portion of the  $^1\text{H}$ -NMR spectrum of m-MeATE.

Figure 19 shows the electron ionization mass spectrum (EI-MS) of m-MeATE (molecular weight 383). The mass to charge value (m/e) of 368 represents the mass of the molecular ion ( $M^+$ ) - 15 ( $CH_3$ ).

The invention is more closely described by the following examples.

#### 5 Example 1

##### Isolation of human scFv antibody fragments specific for the ED-B domain of fibronectin from a antibody phage-display library

A human antibody library was cloned using VH (DP47; Tomlinson et al. (1992). J. Mol. Biol., 227, 776-798.) and Vk (DPK22; Cox et al. (1994). Eur. J. Immunol., 24, 827-836) germline genes (see Figure 1 for the cloning and amplification strategy). The VH component of the library was created using partially degenerated primers (Figure 1) in a PCR-based method to introduce random mutations at positions 95-98 in CDR3. The VL component of the library was generated in the same manner, by the introduction of random mutations at positions 91, 93, 94 and 96 of CDR3. PCR reactions were performed as described (Marks et al. (1991). J. Mol. Biol., 222, 581-597). VH-VL scFv fragments were constructed by PCR assembly (Figure 1; Clackson et al. (1991). Nature, 352, 624-628), from gel-purified VH and VL segments. 30µg of purified VH-VL scFv fragments were double digested with 300 units each of NcoI and NotI, then ligated into 15 µg of NotI/NcoI digested pDN332 phagemid vector. pDN332 is a derivative of phagemid pHEN1 (Hoogenboom et al. (1991). Nucl. Acids Res., 19, 4133-4137), in which the sequence between the NotI site and the amber codon preceding the gene III has been replaced by the following sequence, coding for the D3SD3-FLAG-His6 tag (Neri et al. (1996). Nature Biotechnology, 14, 385-390):

25

```

      NotI      D  D  D  S  D  D  D
Y   K   D   D
5' - GCG GCC GCA GAT GAC GAT TCC GAC GAT GAC TAC AAG GAC GAC

```

30

```

      D  D  K  H  H  H  H  H  H  amber
GAC GAC AAG CAC CAT CAC CAT CAC CAT TAG - 3'

```

Transformations into TG1 E.coli strain were performed according to Marks et al. (1991. J. Mol. Biol., 222, 581-597) and phages were prepared according to

standard protocols (Nissim et al. (1991). *J. Mol. Biol.*, 222, 581-597). Five clones were selected at random and sequenced to check for the absence of pervasive contamination.

Recombinant fibronectin fragments ED-B and 7B89, containing one and four type  
 5 III homology repeats respectively, were expressed from pQE12-based expression vectors (Qiagen, Chatsworth, CA, USA) as described (Carnemolla et al. (1996). *Int. J. Cancer*, 68, 397-405).

Selections against recombinant ED-B domain of fibronectin (Carnemolla et al. (1996). *Int. J. Cancer*, 68, 397-405, Zardi et al. (1987). *EMBO J.*, 6, 2337-2342)  
 10 were performed at 10 nM concentration using the antigen biotinylated with biotin disulfide N-hydroxysuccinimide ester (reagent B-4531; Sigma, Buchs, Switzerland; 10) and eluted from a 2D gel, and streptavidin-coated Dynabeads capture (Dyna, Oslo, Norway). 1013 phages were used for each round of panning, in 1 ml reaction. Phages were incubated with antigen in 2% milk/PBS (MPBS) for 10  
 15 minutes. To this solution, 100 µl Dynabeads (10 mg/ml; Dynal, Oslo, Norway), preblocked in MPBS, were added. After 5 min. mixing, the beads were magnetically separated from solution and washed seven times with PBS-0.1% Tween-20 (PBST) and three times with PBS. Elution was carried out by incubation for 2 min. with 500 µl 50 mM dithiothreitol (DTT), to reduce the disulfide bridge  
 20 between antigen and biotin. Beads were captured again, and the resulting solution was used to infect exponentially growing TG1 E.coli cells. After three rounds of panning, the eluted phage was used to infect exponentially-growing HB2151 E.coli cells and plated on (2xTY + 1% glucose + 100 µg/ml ampicillin) - 1.5% agar plates. Single colonies were grown in 2xTY + 0.1% glucose + 100 µg/ml ampicillin, and  
 25 induced overnight at 30 degrees with 1 mM IPTG to achieve antibody expression. The resulting supernatants were screened by ELISA using streptavidin-coated microtitre plates treated with 10 nM biotinylated-ED-B, and anti-FLAG M2 antibody (IBI Kodak, New Haven, CT) as detecting reagent. 32% of screened clones were positive in this assay and the three of them which gave the strongest ELISA signal  
 30 (E1, A2 and G4) were sequenced and further characterised.

ELISA assays were performed using biotinylated ED-B recovered from a gel spot, biotinylated ED-B that had not been denatured, ED-B linked to adjacent fibronectin

domains (recombinant protein containing the 7B89 domains), and a number of irrelevant antigens. Antibodies E1, A2 and G4 reacted strongly and specifically with all three ED-B containing proteins. This, together with the fact that the three recombinant antibodies could be purified from bacterial supernatants using an ED-B affinity column, strongly suggests that they recognise an epitope present in the native conformation of ED-B. No reaction was detected with fibronectin fragments which did not contain the ED-B domain (data not shown).

In order to test whether the antibodies isolated against a gel spot had a good affinity towards the native antigen, real-time interaction analysis was performed using surface plasmon resonance on a BIAcore instrument as described (Neri et al. (1997) *Nature Biotechnol.*, 15, 1271-1275). Monomeric fractions of E1, A2 and G4 scFv fragments bound to ED-B with affinity in the  $10^7$  -  $10^8$  M<sup>-1</sup> range (Table 1).

As a further test of antibody specificity and usefulness, a 2D-PAGE immunoblot was performed, running on gel a lysate of the human melanoma cell line COLO-38, to which minute amounts of the ED-B containing recombinant 7B89 protein had been added (Figure 2). ScFv(E1) stained strongly and specifically only the 7B89 spot.

Antibodies E1, A2 and G4 were used to immunolocalise ED-B containing fibronectin (B-FN) in cryostat sections of glioblastoma multiforme, an aggressive human brain tumour with prominent angiogenetic processes. Figure 3 shows serial sections of glioblastoma multiforme, with the typical glomerulus-like vascular structures stained in red by the three antibodies. Immunostaining of sections of glioblastoma multiforme samples frozen in liquid nitrogen immediately after removal by surgical procedures, was performed as described (Carnemolla et al. (1996). *Int. J. Cancer*, 68, 397-405, Castellani et al. (1994). *Int. J. Cancer*, 59, 612-618). In short, immunostaining was performed using M2-anti-FLAG antibody (IBI Kodak), biotinylated anti-mouse polyclonal antibodies (Sigma), a streptavidin-biotin alkaline phosphatase complex staining kit (BioSpa, Milan, Italy) and naphthol-AS-MX-phosphate and fast-red TR (Sigma). Gill's hematoxylin was used as a counter-stain, followed by mounting in glycergel (Dako, Carpinteria, CA) as previously reported (Castellani et al. (1994). *Int. J. Cancer*, 59, 612-618).



Using similar techniques and the antibody L19 (see next example) we could also specifically stain new-forming blood vessels induced by implanting in the rabbit cornea polymer pellets soaked with angiogenic substances, such as vascular endothelial growth factor or phorbol esters.

## 5 Example 2

### Isolation of a human scFv antibody fragment binding to the ED-B with sub-nanomolar affinity

ScFv(E1) was selected to test the possibility of improving its affinity with a limited number of mutations of CDR residues located at the periphery of the antigen binding site (Figure 1A). We combinatorially mutated residues 31-33, 50, 52 and 54 of the antibody VH, and displayed the corresponding repertoire on filamentous phage. These residues are found to frequently contact the antigen in the known 3D-structures of antibody-antigen complexes. The resulting repertoire of  $4 \times 10^8$  clones was selected for binding to the ED-B domain of fibronectin. After two rounds of panning, and screening of 96 individual clones, an antibody with 27-fold improved affinity was isolated (H10; Tables 1 and 2). Similarly to what others have observed with affinity-matured antibodies, the improved affinity was due to slower dissociation from the antigen, rather than by improved  $k_{on}$  values (Schier et al. (1996). *Gene*, 169, 147-155, Ito (1995). *J. Mol. Biol.*, 248, 729-732). The antibody light chain is often thought to contribute less to the antigen binding affinity as supported by the fact that both natural and artificial antibodies devoid of light chain can still bind to the antigen (Ward et al. (1989) *Nature*, 341, 544-546, Hamers-Casterman et al. (1993). *Nature*, 363, 446-448). For this reason we chose to randomise only two residues (32 and 50) of the VL domain, which are centrally located in the antigen binding site (Figure 1a) and often found in 3D structures to contact the antigen. The resulting library, containing 400 clones, was displayed on phage and selected for antigen binding. From analysis of the dissociation profiles using real-time interaction analysis with a BIAcore instrument (Jonsson et al. (1991). *BioTechniques*, 11, 620-627) and  $k_{off}$  measurements by competition experiments with electrochemiluminescent detection a clone (L19) was identified, that bound to the ED-B domain of fibronectin with a  $K_d = 54$  pM (Tables 1 and 2).

Affinity maturation experiments were performed as follows. The gene of scFv(E1) was PCR amplified with primers LMB1bis (5'-GCG GCC CAG CCG GCC ATG GCC GAG-3') and DP47CDR1for (5'-GA GCC TGG CGG ACC CAG CTC ATM NNM NNM NNGCTA AAG GTG AAT CCA GAG GCT G-3') to introduce random mutations at positions 31-33 in the CDR1 of the VH (for numbering: 28), and with primers DP47CDR1back (5'-ATG AGC TGG GTC CGC CAG GCT CC-3') and DP47CDR2for (5'-GTC TGC GTA GTA TGT GGT ACC MNN ACT ACC MNN AAT MNN TGA GAC CCA CTC CAG CCC CTT-3') to randomly mutate positions 50,52,54 in CDR2 of the VH. The remaining fragment of the scFv gene, covering the 3'- portion of the VH gene, the peptide linker and the VL gene, was amplified with primers DP47CDR2back (5'-ACA TAC TAC GCA GAC TCC GTG AAG-3') and JforNot (5'-TCA TTC TCG ACT TGC GGC CGC TTT GAT TTC CAC CTT GGT CCC TTG GCC GAA CG-3') (94°C 1 min, 60 C 1 min, 72 C 1 min). The three resulting PCR products were gel purified and assembled by PCR (21) with primers LMB1bis and JforNot (94°C 1 min, 60 C 1 min, 72 C 1 min). The resulting single PCR product was purified from the PCR mix, double digested with NotI/NcoI and ligated into NotI/NcoI digested pDN332 vector. Approximately 9 µg of vector and 3 µg of insert were used in the ligation mix, which was purified by phenolisation and ethanol precipitation, resuspended in 50 µl of sterile water and electroporated in electrocompetent TGI E.coli cells. The resulting affinity maturation library contained  $4 \times 10^8$  clones. Antibody-phage particles, produced as described (Nissim et al. (1994). EMBO J., 13, 692-698) were used for a first round of selection on 7B89 coated imunotube (Carnemolla et al. (1996). Int. J. Cancer, 68, 397-405). The selected phages were used for a second round of panning performed with biotinylated ED-B, followed by capture with streptavidin coated magnetic beads (Dynal, Oslo, Norway; see previous paragraph). After selection, approximately 25% of the clones were positive in soluble ELISA (see previous chapter for experimental protocol). From the candidates positive in ELISA, we further identified the one (H10; Table 1) with lowest koff by BIAcore analysis (Jonsson et al. (1991), BioTechniques, 11, 620-627).

The gene of scFv(H10) was PCR amplified with primers LMB1bis and DPKCDR1for (5'-G TTT CTG CTG GTA CCA GGC TAA MNN GCT GCT GCT

AAC ACT CTG ACT G) to introduce a random mutation at position 32 in CDR1 of the VL (for numbering: Chothia and Lesk (1987) *J.Mol.Biol.*, 196, 901-917), and with primers DPKCDR1back (5'-TTA GCC TGG TAC CAG CAG AAA CC-5') and DPKCDR2for (5'-GCC AGT GGC CCT GCT GGA TGC MNN ATA GAT GAG GAG  
5 CCT GGG AGC C-3') to introduce a random mutation at position 50 in CDR2 of the VL. The remaining portion of the scFv gene was amplified with oligos DPKCDR2back (5'-GCA TCC AGC AGG GCC ACT GGC-3') and JforNot (94C 1 min, 60 C 1 min, 72 C 1 min) The three resulting products were assembled, digested and cloned into pDN332 as described above for the mutagenesis of the  
10 heavy chain. The resulting library was incubated with biotinylated ED-B in 3% BSA for 30 min., followed by capture on a streptavidin-coated microtitre plate (Boehringer Mannheim GmbH, Germany) for 10 minutes. The phages were eluted with a 20 mM DTT solution (1,4-Dithio-DL-threitol, Fluka) and used to infect exponentially growing TG1 cells.

15 Analysis of ED-B binding of supernatants from 96 colonies by ELISA and by BIAcore allowed the identification of clone L19. Anti-ED-B E1, G4, A2, H10 and L19 scFv antibody fragments selectively stain new-forming blood vessels in sections of aggressive tumours (Figure 3).

The above mentioned anti-ED-B antibody fragments were then produced  
20 inoculating a single fresh colony in 1 liter of 2xTY medium as previously described in Pini et al. ((1997), *J. Immunol. Meth.*, 206, 171-182) and affinity purified onto a CNBr-activated sepharose column (Pharmacia, Uppsala, Sweden), which had been coupled with 10 mg of ED-B containing 7B89 recombinant protein (Carnemolla et al. (1996). *Int. J. Cancer*, 68, 397-405). After loading, the column  
25 was washed with 50 ml of equilibration buffer (PBS, 1 mM EDTA, 0.5 M NaCl). Antibody fragments were then eluted with triethylamine 100 mM, immediately neutralised with 1M Hepes, pH 7, and dialysed against PBS. Affinity measurements by BIAcore were performed with purified antibodies as described (Neri et al. (1997). *Nature Biotechnol.*, 15 1271-1275) [Figure 4]. Band-shift  
30 analysis was performed as described (Neri et al. (1996). *Nature Biotechnology*, 14, 385-390), using recombinant ED-B fluorescently labelled at the N-terminal extremity (Carnemolla et al. (1996). *Int. J. Cancer*, 68, 397-405, Neri et al. (1997) .

Nature Biotechnol., 15 1271-1275) with the infrared fluorophore Cy5 (Amersham) [Figure 4]. BIAcore analysis does not always allow the accurate determination of kinetic parameters for slow dissociation reactions due to possible rebinding effects, baseline instability and long measurement times needed to ascertain that the dissociation phase follows a single exponential profile. We therefore performed measurements of the kinetic dissociation constant  $k_{off}$  by competition experiments (Neri et al. (1996), Trends in Biotechnol., 14, 465-470) [Figure 4]. In brief, anti-ED-B antibodies (30 nM) were incubated with biotinylated ED-B (10 nM) for 10 minutes, in the presence of M2 anti-FLAG antibody (0,5 µg/ml) and polyclonal anti-mouse IgG (Sigma) which had previously been labelled with a rutenium complex as described (Deaver, D. R. (1995). Nature, 377, 758-760). To this solution, in parallel reactions, unbiotinylated ED-B (1 µM) was added at different times. Streptavidin-coated dynabeads, diluted in Origen Assay Buffer (Deaver, D.R. (1995). Nature, 377, 758-760) were then added (20 µl, 1 mg/ml), and the resulting mixtures analysed with a ORIGIN Analyzer (IGEN Inc. Gaithersburg, MD USA). This instrument detects an electrochemiluminescent signal (ECL) which correlates with the amount of scFv fragment still bound to the biotinylated ED-B at the end of the competition reaction. Plot of the ECL signal versus competition time yields a profile, that can be fitted with a single exponential with characteristic constant  $k_{off}$  [Figure 4; Table 2].

### Example 3

#### Targeting tumours with a high-affinity radiolabelled scFv specific for the ED-B domain of fibronectin

Radioiodinated scFv(L19) or scFv(D1.3) (an irrelevant antibody specific for hen egg lysozyme) were injected intravenously in mice with subcutaneously implanted murine F9 teratocarcinoma, a rapidly growing aggressive tumour. Antibody biodistributions were obtained at different time points (Figure 4). ScFv(L19) and scFv(D1.3) were affinity purified on an antigen column (Neri et al. (1997, Nature Biotechnol. 15, 1271-1273) and radiolabelled with iodine-125 using the Iodogen method (Pierce, Rockford, IL, USA). Radiolabelled antibody fragments retained > 80% immunoreactivity, as evaluated by loading the radiolabelled antibody onto an antigen column, followed by radioactive counting of the flow-through and eluate

fractions. Nude mice (12 weeks old Swiss nudes, males) with subcutaneously-implanted F9 murine teratocarcinoma (Neri et al. (1997) Nature Biotechnol. 15, 1271-1273) were injected with 3 µg (3-4 µCi) of scFv in 100 µl saline solution. Tumour size was 50-250 mg, since larger tumours tend to have a necrotic centre.

5 However, targeting experiments performed with larger tumours (300-600 mg) gave essentially the same results. Three animals were used for each time point. Mice were killed with humane methods, and organs weighed and radioactively counted. Targeting results of representative organs are expressed as percent of the injected dose of antibody per gram of tissue (% ID / g). ScFv(L19) is rapidly eliminated  
10 from blood through the kidneys; unlike conventional antibodies, it does not accumulate in the liver or other organs. Eight percent of the injected dose per gram of tissue localises on the tumour already three hours after injection; the subsequent decrease of this value is due to the fact that the tumour doubles in size in 24-48 hours. Tumour:blood ratios at 3, 5 and 24 hours after injection were  
15 1.9, 3.9 and 11.8 respectively for L19, but always below 1.0 for the negative control antibody.

Radiolabelled scFv(L19) preferentially localises on tumours already few hours after injection, suggesting its usefulness for the immunoscintigraphic detection of angiogenesis in patients.

#### 20 Example 4

##### Anti-ED-B antibodies selectively stain newly-formed ocular blood vessels

Angiogenesis, the formation of new blood vessels from pre-existing ones, is a characteristic process which underlies many diseases, including cancer and the majority of ocular disorders which result in loss of vision. The ability to selectively  
25 target and occlude neovasculature will open diagnostic and therapeutic opportunities.

We investigated whether B-FN is a specific marker of ocular angiogenesis and whether antibodies recognising B-FN could selectively target ocular neovascular structures in vivo upon systemic administration. To this aim we stimulated  
30 angiogenesis in the rabbit cornea, which allows the direct observation of new-blood vessels, by surgically implanting pellets containing vascular endothelial growth factor or a phorbol ester (Figure 7). Sucralfate (kind gift of Merck,

Darmstadt, Germany) / hydron pellets containing either 800 ng vascular endothelial growth factor (Sigma) or 400 ng phorbol 12-myristate 13-acetate («PMA»; Sigma) were implanted in the cornea of New Zealand White female rabbits as described [D'Amato, R.J., et al., *Proc. Natl. Acad. Sci. USA* 91, 4082-4085 (1994)]. Angiogenesis was induced by both factors. Rabbits were monitored daily. With both inducers newly formed blood vessels were strongly ED-B-positive in immunohistochemistry. For all further experiments, PMA pellets were used. Immunohistochemical studies showed that L19 strongly stains the neovasculature induced in the rabbit cornea (Fig. 8; 9a), but not pre-existing blood vessels of the eye (Fig. 9b, c) and of other tissues (data not shown). Immunohistochemistry was performed as described [Carnemolla, B. *et al.*, *Int. J. Cancer* 68, 397-405 (1996)].

#### Example 5

The human antibody fragment L19, binding to the ED-B with sub-nanomolar affinity, targets ocular angiogenesis *in vivo*

Using the rabbit cornea model of angiogenesis described in the previous example, and an immunophotodetection methodology [Neri, D. *et al.*, *Nature Biotechnol.* 15, 1271-1275 (1997)], we demonstrated that L19, chemically coupled to the red fluorophore Cy5, but not the antibody fragment (HyHEL-10)-Cy5 directed against an irrelevant antigen (Fig. 10a,b), selectively targets ocular angiogenesis upon intravenous injection. Fluorescent staining of growing ocular vessels was clearly detectable with L19 immediately after injection, and persisted for at least two days analogous to previous observations with tumour angiogenesis. Subsequent *ex vivo* immunofluorescent microscopic analysis on cornea sections confirmed the localisation of L19, but not of HyHEL-10, around vascular structures (Fig. 10c,d).

The demonstration of the antibody-based selective targeting of ocular neovascularisation, together with the reactivity of anti-B-FN antibodies in different species, warrants future clinical investigations. Immunofluorescence imaging could be useful for the early detection of ocular angiogenesis in risk patients, before lesions become manifest in fluoroangiography.

Some methodological details:

For *ex vivo* immunofluorescence and for some H/E stainings, corneas were fixed in 4% paraformaldehyde in PBS before embedding. Fluorescence photodetection

experiments were performed with rabbits sedated using 5 mg/kg Acepromazin. For targeting experiments, 3.5 mg of scFv(L19)<sub>1</sub>-Cy5<sub>0.66</sub> and 2.8 mg of scFv(HyHEL-10)<sub>1</sub>-Cy5<sub>0.83</sub> were injected intravenously in each rabbit (injection time = 15 min). A strong fluorescence in the corneal neovasculature was observed already immediately after injection of L19, but not of HyHEL-10, and persisted for several hours. As an additional test of specificity, rabbits injected the previous day with scFv(HyHEL-10)-Cy5 and negative in the fluorescence photodetection, were injected the next day with scFv(L19)-Cy5, and showed a strong fluorescent staining of corneal angiogenesis.

For fluorescence detection, the eye was illuminated with a tungsten halogen lamp (model Schott KL1500; Zeiss, Jena, Germany) equipped with a Cy5-excitation filter (Chroma, Brattleboro, VT, U.S.A.) and with two light guides whose extremities were placed at approximately 2 cm distance from the eye. Fluorescence was detected with a cooled C-5985 monochrome CCD-camera (Hamamatsu, Hamamatsu-City, Japan), equipped with C-mount Canon Zoom Lens (V6x16; 16-100 mm; 1: 1.9) and a 50 mm diameter Cy5 emission filter (Chroma), placed at 3-4 cm distance from the irradiated eye. Acquisition times were 0.4 s.

Cy5 fluoroangiography experiments were performed with the same experimental set up, but injecting intravenously 0.25 mg Cy5-Tris (the reaction product between Cy5-NHS and tris[hydroxymethyl]aminomethane; injection time = 5 s). Acquisition times were 0.2 s.

Antibody fragments were in scFv format. The purification of scFv(L19) and scFv(HyHEL-10) and their labeling with the N-hydroxysuccinimide (NHS) esters of indocyanine dyes have been described elsewhere [Neri, D. *et al.*, *Nature Biotechnol.* 15, 1271-1275 (1997); Fattorusso, R., *et al.* (1999) *Structure*, 7, 381-390]. Antibody : Cy5 labeling ratios for the two antibodies were 1.5 : 1 and 1.2 : 1, respectively. Cy5-NHS was purchased from Amersham Pharmacia Biotech (Zurich, Switzerland), ovalbumin from Sigma (Buchs, Switzerland).

After the labeling reaction, antibody conjugates were separated from unincorporated fluorophore or photosensitiser using PD-10 columns (Amersham Pharmacia Biotech) equilibrated in 50 mM phosphate, pH 7.4, 100 mM NaCl (PBS). Immunoreactivity of antibody conjugates was measured by affinity

chromatography on antigen columns [Neri, D. *et al.*, *Nature Biotechnol.* 15, 1271-1275 (1997)] and was in all cases > 78%. Immunoconjugates were analysed by sodium dodecyl sulfate polyacrylamide gel electrophoresis and migrated as a band of MW = 30'000 Dalton (purity = 90%).

## 5 Example 6

The human antibody fragment L19, chemically conjugated to the photosensitiser Sn (IV) chlorine e6, selectively targets ocular angiogenesis and mediates its occlusion upon irradiation with red light

To test whether selective vessel ablation could be achieved by virtue of the  
 10 antibody-mediated targeting, we injected rabbits with the L19 antibody fragment or an irrelevant protein that does not localise in newly formed blood vessels (ovalbumin) coupled to the photosensitiser tin (IV) chlorin e<sub>6</sub> (hereafter named «PS»). The eyes of injected animals were irradiated with red light (light dose = 78 J/cm<sup>2</sup>). Representative results are depicted in Figure 11. A striking macroscopic  
 15 difference was observed 16 h after irradiation in rabbits treated with L19-PS (Fig. 11a,b), with coagulation of the corneal neovasculature but not of vessels in the conjunctiva or in other ocular structures. Fluoroangiography with the indocyanine fluorophore Cy5 (Fig. 11c) confirmed vessel occlusion as a characteristic hypofluorescent area. On the contrary, hyperfluorescent areas were observed in  
 20 the leaky neovasculature of non-irradiated eyes (Fig. 11d,h). No macroscopic alteration was detectable in the irradiated vessels of rabbits treated with ovalbumin-PS (Fig. 11e-g), either ophthalmoscopically or by Cy5 fluoroangiography. The effect of irradiation of the targeted L19-PS conjugate at early stages of corneal angiogenesis are shown in Fig. 11i-l. Selectively  
 25 coagulated blood vessels were macroscopically visible in live animals (Fig. 11i,j) and even more evident in animals immediately after euthanasia (Fig. 11k,l).

Photodynamic damage was further investigated using microscopic techniques. After irradiation, vessel occlusion could be detected by standard hematoxylin/eosin (H/E) staining techniques in both non-fixed and paraformaldehyde-fixed cornea  
 30 sections of animals treated with L19-PS (Fig. 11b,f,j), but not of those treated with ovalbumin-PS (Fig. 11a,e,i). Apoptosis in the portion of the cornea targeted by the photosensitiser conjugate was clearly visible in the fluorescent TUNEL assay (Fig.



11c,g), but hardly detectable ink negative controls (Fig. 11d,h). A higher magnification view showed apoptosis of endothelial cells in vascular structures (Fig. 11g). No damage to blood vessels of the iris, sclera and conjunctiva of treated animals could be observed either by TUNEL assay (not shown) or by H/E staining (Fig. 11k,l).

Selective photodynamic ablation of neovasculature promises to be beneficial for the treatment of ocular disorders and of other angiogenesis-related pathologies that are accessible to irradiation using light diffusers or fibre optic techniques. The results of this study clearly demonstrate that ocular neovasculature can be selectively occluded without damaging pre-existing blood vessels and normal tissues.

Some methodological details:

Tin (IV) chlorin  $e_6$  was selected from a panel of photosensitisers, on the basis of their potency, solubility and specificity, after coupling to a rabbit anti-mouse polyclonal antibody (Sigma). These immunoconjugates were screened by targeted photolysis of red blood cells coated with a monoclonal antibody specific for human CD47 (#313441A; Pharmingen, San Diego CA, U.S.A.). Tin (IV) chlorin  $e_6$  was prepared as described [Lu, X.M. *et al.*, *J. Immunol. Methods* 156, 85-99 (1992)]. For coupling to proteins, tin (IV) chlorin  $e_6$  (2 mg/ml) was mixed for 30 min at room temperature in dimethylformamide with a ten-fold molar excess of EDC (N'-3-dimethylaminopropyl-N-ethylcarbodiimide hydrochloride, Sigma) and NHS (N-hydroxysuccinimide, Sigma). The resulting activated mixture was then added to an eight-fold larger volume of protein solution (1 mg/ml) and incubated at room temperature for 1h.

After the labeling reaction, antibody conjugates were separated from unincorporated fluorophore or photosensitiser using PD-10 columns (Amersham Pharmacia Biotech) equilibrated in 50 mM phosphate, pH 7.4, 100 mM NaCl (PBS). Immunoreactivity of antibody conjugates was measured as described in the previous Example.

For photokilling experiments, rabbits were injected intravenously with 12 mg scFv(L19)<sub>1</sub>-tin (IV) chlorin  $e_{6,8}$  or 38 mg ovalbumin<sub>1</sub> – tin (IV) chlorin  $e_{6,36}$ , and kept in the dark for the duration of the experiment. Eight hours after injection,

rabbits were anaesthetised with ketamin (35 mg/kg) / xylazine (5 mg/kg) / acepromazin (1 mg/kg), and one of the two eyes was irradiated for 13 min with a Schott KL1500 tungsten halogen lamp equipped with a Cy5 filter (Chroma) and with two light guides whose extremities were placed at 1 cm distance from the eye.

- 5 The illuminated area was approximately 1 cm<sup>2</sup>, with an irradiation power density of 100 mW/cm<sup>2</sup>, measured using a SL818 photodetector (Newport Corp., Irvine, CA, U.S.A.). No sign of animal discomfort after irradiation was observed. As a preventive measure, rabbits received analgesics after irradiation (buprenorphine 0.03 mg/Kg). To monitor photokilling, eyes were investigated with an
- 10 ophthalmoscope and photographed using a fundus camera KOWA SL-14 (GMP SA, Rennens, Lausanne, Switzerland). Five rabbits were treated with each of the tin (IV) chlorin e<sub>6</sub> conjugates and irradiated in one eye only, the other eye serving as an internal negative control. As additional control, two rabbits were irradiated only, but received no photosensitiser conjugate.
- 15 Immediately after rabbits' euthanasia with an overdose of anaesthetic, eyes were enucleated, corneas removed, then embedded in Tissue Tek (Sakura Finetechnical, Tokyo, Japan) and frozen. For ex vivo immunofluorescence and for some H/E stainings, corneas were fixed in 4% paraformaldehyde in PBS before embedding. Cryostat sections of 5 µm were used for further microscopic analysis.
- 20 Fluorescent TUNEL assays were performed according to manufacturer's instructions (Roche Diagnostic, Rotkreuz, Switzerland).

#### Example 7

##### Conjugation of astatine-211 to human antibody fragment L19 through m-MeATE

- 25 A solution of m-bromobenzoic acid (1 g, 5 mmol) in 25 ml of dry tetrahydrofuran (THF) is placed in a 250 ml, two-necked round bottom flask, maintained under nitrogen atmosphere and cooled to – 75 °C using (ether:dry ice) bath. To the above, 6.25 ml of n-buthyl lithium (1.6M solution in hexane) is added slowly over 25 min. The dilithio anion thus generated is stirred for an additional 10 min. Still under a nitrogen atmosphere, trimethylstannyl chloride (1.09 mg, 5.47 mmol)
- 30 dissolved in 10 ml dry THF is added over 20 min to the reaction mixture. The cooling bath is removed and the reaction is slowly brought to room temperature (RT) and stirring is kept for 1 hour. The reaction is quenched by addition of water

(10 ml) and extracted three times with 100 ml of diethyl ether. The organic phase is washed with 5% NaHCO<sub>3</sub> (2 x 25 ml) and water (2 x 20 ml). After drying over MgSO<sub>4</sub>, it is concentrated on a rotary evaporator. Thin layer chromatography (TLC) is performed on analytical, pre-coated silica gel plastic plates using the following mobile phase: Hexane:ethylacetate(EtOAc):acetic acid (AcOH) (70:29.7:0.3). 3-(trimethylstannyl) benzoate (R<sub>f</sub> = 0.46) is purified by gravimetric chromatography using a silica gel 60 column (40-63  $\mu$ , 200 x 3 mm) eluted with the same phase above reported. We obtain 100 mg (0.35 mmol) of product, in 7% yield as an oil. The assigned structure (<sup>1</sup>H-NMR) is reported in Figure 17a,b.

To the stannyl ester resuspended in THF (10 ml), N-hydroxy-succinimide (48.34 mg, 0.42 mmol) and dicyclohexylcarbodiimide (86.66 mg, 0.42 mmol) are added and stirred overnight at room temperature. Precipitated dicyclohexylurea is filtered off and the solvent is evaporated on a rotary evaporator to give an oil. The desired m-MeATE (R<sub>f</sub> = 0.34) is isolated by gravimetric chromatography with Hexane:EtOAc (2:1) using a silica gel 60 column. After evaporation of the solvent we obtain 92.3 mg (0.241 mmol) of m-MeATE in 68.8% relative yield. The assigned structure is confirmed by <sup>1</sup>H-NMR and Mass Spectroscopy (Figures 18a,b and 19). This bifunctional compound is used to couple scFv(L19) to the alpha-emitting radionuclide Astatine-211.

In a glove-box previously inflated with inert gas, 1.9 mg of m-MeATE (5  $\mu$ mol) and *tert* -butryl hydroperoxide (20  $\mu$ mol) are added to the chloroform trap containing 1 mCi <sup>211</sup>At anion. The reaction is kept at room temperature for 15 minutes and the mixture is purified using a disposable Sep-Pak silica gel cartridge. The reaction mixture is added to 300  $\mu$ l of Hexane and loaded on the column previously equilibrated with Hexane. Following washing with Hexane (40 ml) and 8% ethylacetate in Hexane (25 ml), the product N-succinimidyl 3-<sup>211</sup>At-benzoate is isolated in 30% ethylacetate in Hexane (ca. 15 ml). The radionuclide incorporation in the bifunctional agent m-MeATE is measured using an automated gamma counter with an energy window set to include the Polonium K X-rays emitted in the decay of <sup>211</sup>At. The eluted fraction is evaporated and resuspended in dimethyl sulfoxide (100  $\mu$ l) and then added to 200  $\mu$ l of borate buffer (pH = 8.5) containing 13 nmoles of scFv (L19). The reaction is stirred at room temperature for 30

minutes and the L19-<sup>211</sup>At conjugate is purified using a PD-10 disposable gel filtration column. Antibody immunoreactivity after labeling is evaluated by loading an aliquot of radiolabeled sample onto 200  $\mu$ l of ED-B-Sepharose resin (capacity, > 2.5 mg ED-B/ml resin) on a pasteur pipette, followed by radioactive counting of the flow-through and eluate fractions. Immunoreactivity, defined as the ratio between the counts of the eluted protein and the sum of the counts of the eluted and flow-through fractions, is > 80%.

Table 1:

Sequences of selected anti-ED-B antibody clones

		VH chain			VL chain		
5	Clone	31-33*	50-54*	95-98*	32*	50*	91-96*
	A2	SYA	AISGSG	GLSI	Y	G	NGWYPW
	G4	SYA	AISGSG	SFSF	Y	G	GGWLPY
10	E1	SYA	AISGSG	FPFY	Y	G	TGRIPP
	H10	SFS	SIRGSS	FPFY	Y	G	TGRIPP
	L19	SFS	SIRGSS	FPFY	Y	Y	TGRIPP

15

Relevant amino acid positions (\*: numbering according to Tomlinson et al. (1995) EMBO J., 14, 4628-4638) of antibody clones isolated from the designed synthetic libraries. Single amino acid codes are used according to standard IUPAC nomenclature.

20

Table 2:

Affinities of anti-ED-B scFv fragments

	Clone	$k_{on}$ ( $s^{-1}M^{-1}$ )	$k_{off}$ ( $s^{-1}$ ) <sup>B</sup>	$k_{off}$ ( $s^{-1}$ ) <sup>C</sup>	$K_d$ (M)*
5	A2	$1.5 \times 10^5$	$2.8 \times 10^{-3}$	-	$1.9 \times 10^{-8}$
	G4	$4.0 \times 10^4$	$3.5 \times 10^{-3}$	-	$8.7 \times 10^{-8}$
10	E1	$1.6 \times 10^5$	$6.5 \times 10^{-3}$	-	$4.1 \times 10^{-8}$
	H10	$6.7 \times 10^4$	$5.6 \times 10^{-4}$	$9.9 \times 10^{-5}$	$1.5 \times 10^{-9}$
	L19	$1.1 \times 10^5$	$9.6 \times 10^{-5}$	$6.0 \times 10^{-6}$	$5.4 \times 10^{-11}$

\*)  $K_d = k_{off} / k_{on}$ . For the high-affinity binders H10 and L19,  $k_{off}$  values from BIAcore experiments are not sufficiently reliable due to effects of the negatively-charged carboxylated solid dextran matrix;  $K_d$  values are therefore calculated from  $k_{off}$  measurements obtained by competition experiments (Experimental Procedures).

$k_{off}$ , kinetic dissociation constant;  $k_{on}$ , kinetic association constant;  $K_d$ , dissociation constant. B = measured on the BIAcore; C = measured by competition with electrochemiluminescent detection. Values are accurate to +/- 50%, on the basis of the precision of concentration determinations.

## CLAIMS

1. An antibody with specific affinity for a characteristic epitope of the ED-B domain of fibronectin, wherein the antibody has improved affinity to said ED-B epitope.
2. The antibody according to claim 1, wherein the affinity is in the subnanomolar range.
3. The antibody according to claim 1, wherein the antibody recognizes ED-B(+) fibronectin.
4. The antibody according to claim 1, wherein said antibody is in the scFv format.
5. The antibody according to claim 4, the antibody being a recombinant antibody.
6. The antibody according to claim 4, wherein the affinity is improved by introduction of a limited number of mutations in its CDR residues.
7. The antibody according to claim 6, wherein the residues are residues 31-33, 50, 52 and 54 of VH and two residues 32 and 50 of its VL domain which have been mutated.
8. The antibody according to claim 1, wherein the antibody binds the ED-B domain of fibronectin with a Kd of 27 to 54 pM, most preferably with a Kd of 54 pM.
9. The antibody according to claim 1, being the antibody L19.
10. The antibody according to claim 1 with the following amino acid sequence:  
VH  
EVQLLES GGG LVQP GGS LRL SCAAS GFTFS  
SFSMSWVRQA PGK GLEWVSS ISGSS GTTYY  
ADSVKGRFTI SRDNS KNTLY LQMNS LRAED  
TAVYYCAKPF PYFDYWGQGT LTVSS  
linker  
GDGSSGGSGGASTG  
VL  
EIVLTQSPGT LSLSPGERAT LSCRASQSVS  
SSYLAWYQQK PGQAPRL LIY YASSRATGIP  
DRFSGSGSGT DFTLTISRLE PEDFAVYYCQ  
QTGRIPPTFG QGTKVEIK
11. The antibody according to claim 1, wherein the antibody is a functionally equivalent variant form of L19.
12. The antibody according to claim 9, wherein the antibody is radiolabelled.
13. The antibody according to claim 12, wherein the antibody is radioiodinated.

14. Method for rapid angiogenesis targeting wherein an antibody with specific affinity for a characteristic epitope of the ED-B domain of fibronectin, the antibody having improved affinity to said ED-B domain, is used.
15. Method according to claim 14 for immunoscintigraphic detection of angiogenesis.
16. Method according to claim 15 for detecting diseases characterized by vascular proliferation such as diabetic retinopathy, age-related macular degeneration or tumours.
17. Method according to claim 14, wherein the antibody localizes the respective tissue three to four hours, most preferably 3 hours after its injection.
18. A diagnostic kit comprising an antibody with specific affinity for a characteristic epitope of the ED-B domain of fibronectin, said antibody having improved affinity to said ED-B domain and one or more reagents necessary for detecting angiogenesis.
19. Method for diagnosis and therapy of tumours and diseases characterized by vascular proliferation wherein an antibody with specific affinity for a characteristic epitope of the ED-B domain of fibronectin, said antibody having improved affinity to said ED-B domain, is used.
20. Conjugates comprising an antibody according to Claim 1 and a molecule capable of inducing blood coagulation and blood vessel occlusion.
21. Conjugates according to claim 20 wherein the molecule capable of inducing blood coagulation and blood vessel occlusion is a photoactive molecule.
22. Conjugates according to claim 21 wherein the photoactive molecule is a photosensitizer.
23. Conjugates according to claim 22 wherein the photosensitizer absorbs at wavelength above 600 nm.
24. Conjugates according to claim 22 wherein the photosensitizer is a derivative of tin (IV) chloride.
25. Conjugates according to claim 20 wherein the molecule capable of inducing blood coagulation and blood vessel occlusion is a radionuclide.
26. Conjugates according to claim 25 wherein the radionuclide is an  $\alpha$ - or  $\beta$ -emitting radionuclide.



27. Conjugates according to Claim 26 the  $\alpha$ -emitting radionuclide is astatine-211, bismuth-212, bismuth-213.

28. Conjugates according to claim 20 wherein the molecule capable of inducing blood coagulation and blood vessel occlusion is represented by a photosensitizer and a radionuclide.

29. Method for the treatment of angiogenesis-related pathologies wherein a conjugate according to claim 20 is injected.

30. Method for the treatment of angiogenesis-related pathologies wherein a conjugate according to claim 22 is injected, followed by irradiation.

31. Method according to claim 30 wherein the angiogenesis-related pathology treated is caused by or associated with ocular angiogenesis.

32. Method for the treatment of angiogenesis-related pathologies wherein a conjugate according to claim 25 is injected.

33. Method according to claim 32 wherein the radionuclide is astatine-211.

34. Method for the treatment of angiogenesis-related pathologies wherein a conjugate according to claim 28 is injected.

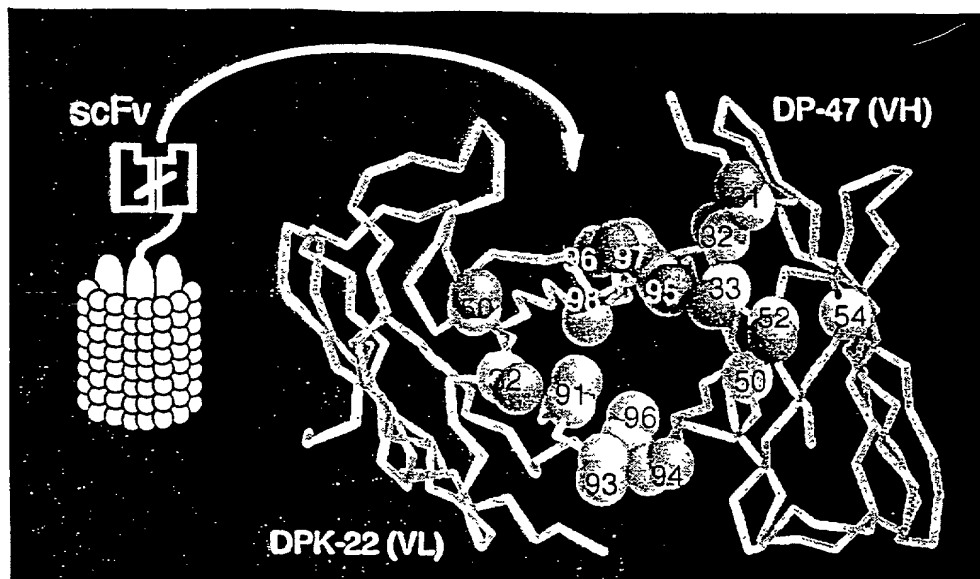
35. 3-(trimethylstannyl)benzoic acid

SPECIFIC BINDING MOLECULES FOR SCINTIGRAPHY, CONJUGATES  
CONTAINING THEM AND THERAPEUTIC METHOD FOR TREATMENT OF  
ANGIOGENESIS

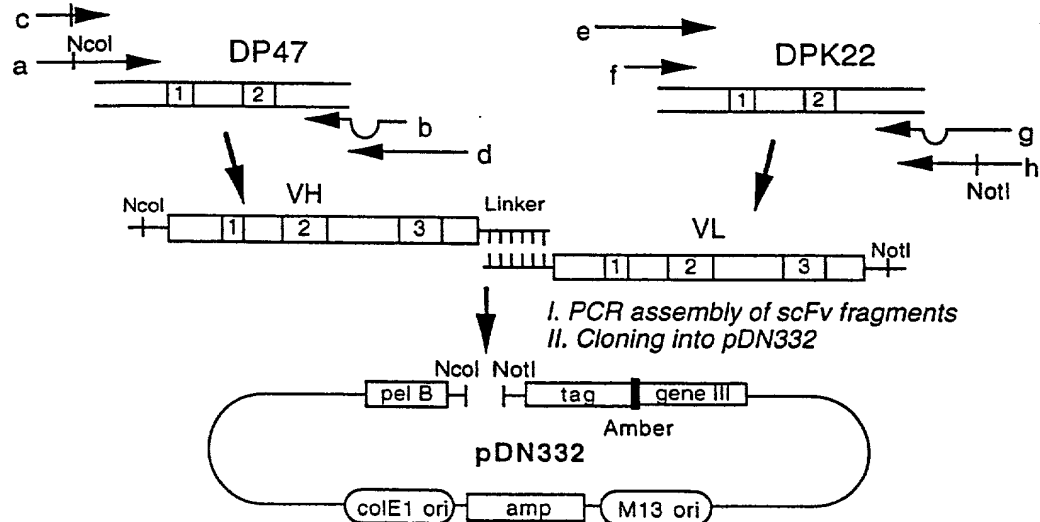
Abstract of the disclosure

- 5 The present invention relates to antibodies with sub-nanomolar affinity specific for  
a characteristic epitope of the ED-B domain of fibronectin, a marker of  
angiogenesis. Furthermore, it relates to the use of radiolabelled high affinity anti  
ED-B antibodies for detecting new-forming blood vessels in vivo and a diagnostic  
10 kit comprising comprising said antibody. Furthermore, it relates to conjugates  
comprising said antibodies and a suitable photoactive molecules (e.g. an  
appropriately chosen photosensitizer or radionuclide), and their use for the  
selective light-mediated occlusion of new blood vessels.

A)



B)



VH primers:

a	DP47baNco	GCG GCC CAG CAT GCC ATG GCC GAG GTG CAG CTG TTG GAG TCT GGG
b	CDR3for	GGT TCC CTG GCC CCA GTA GTC AAA MNN MNN MNN MNN TTT CGC ACA GTA ATA TAC G
c	VHpullth	GCG GCC CAG CAT GCC ATG GCC GAG
d	Jassm	CCC GCT ACC GCC ACT GGA CCC ATC GCC ACT CGA GAC GGT GAC CAG GGT TCC CTG GCC CCA GTA GTC

VL primers:

e	DPK22assm	GAT GGG TCC AGT GGC GGT AGC GGG GGC GCG TCG ACT GGC GAA ATT GTG TTG ACG CAG TCT CC
f	DPK3for	CAC CTT GGT CCC TTG GCC GAA CGT MNN CGG MNN MNN ACC MNN CTG CTG ACA GTA ATA CAC TGC
g	Jfornot	GAG TCA TTC TCG ACT TGC GGC CGC TTT GAT TTC CAC CTT GGT CCC TTG GCC GAA CG
h	pullth	GAT GGG TCC AGT GGC GGT AGC GGG

Figure 1

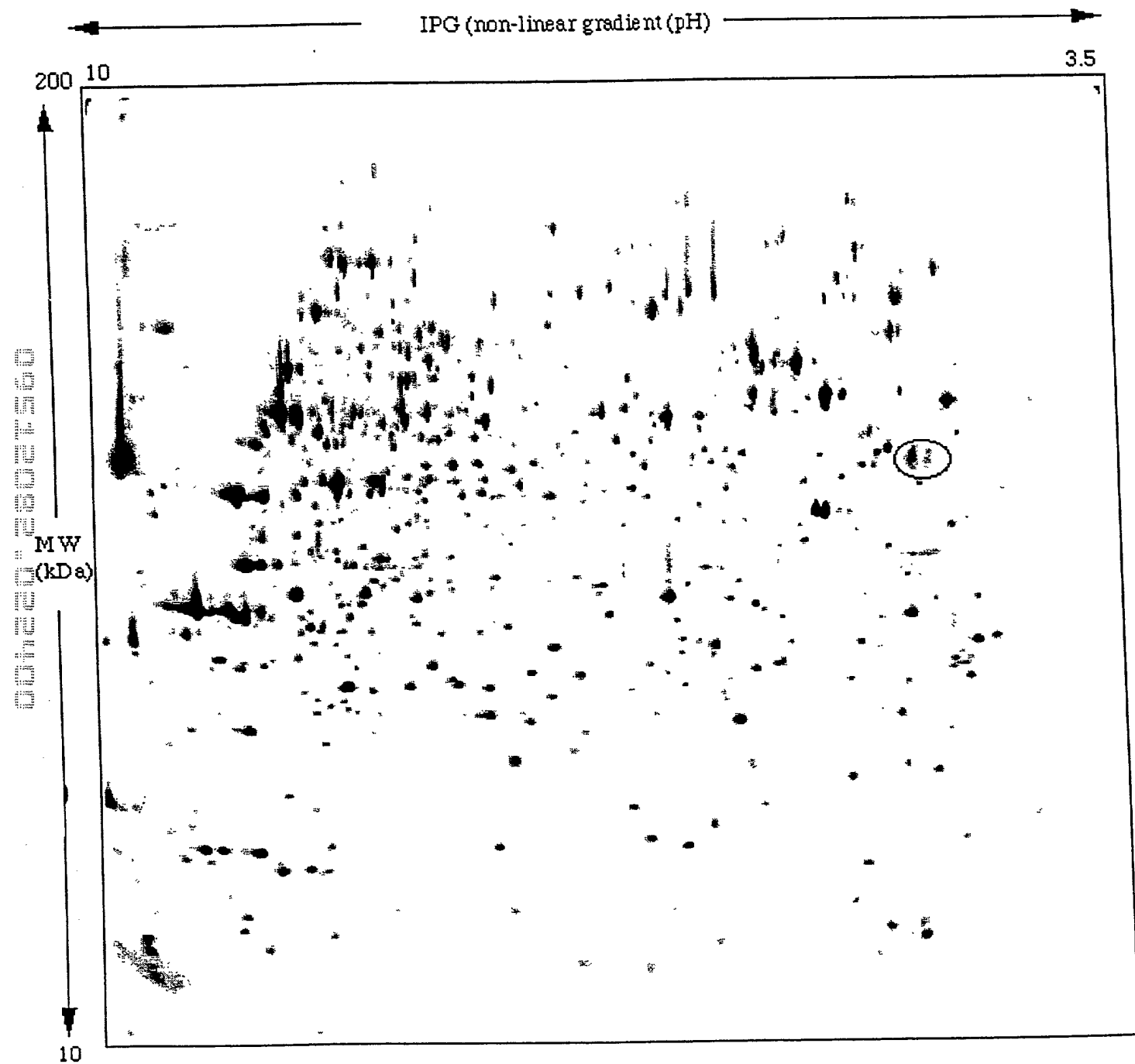


Figure 2A

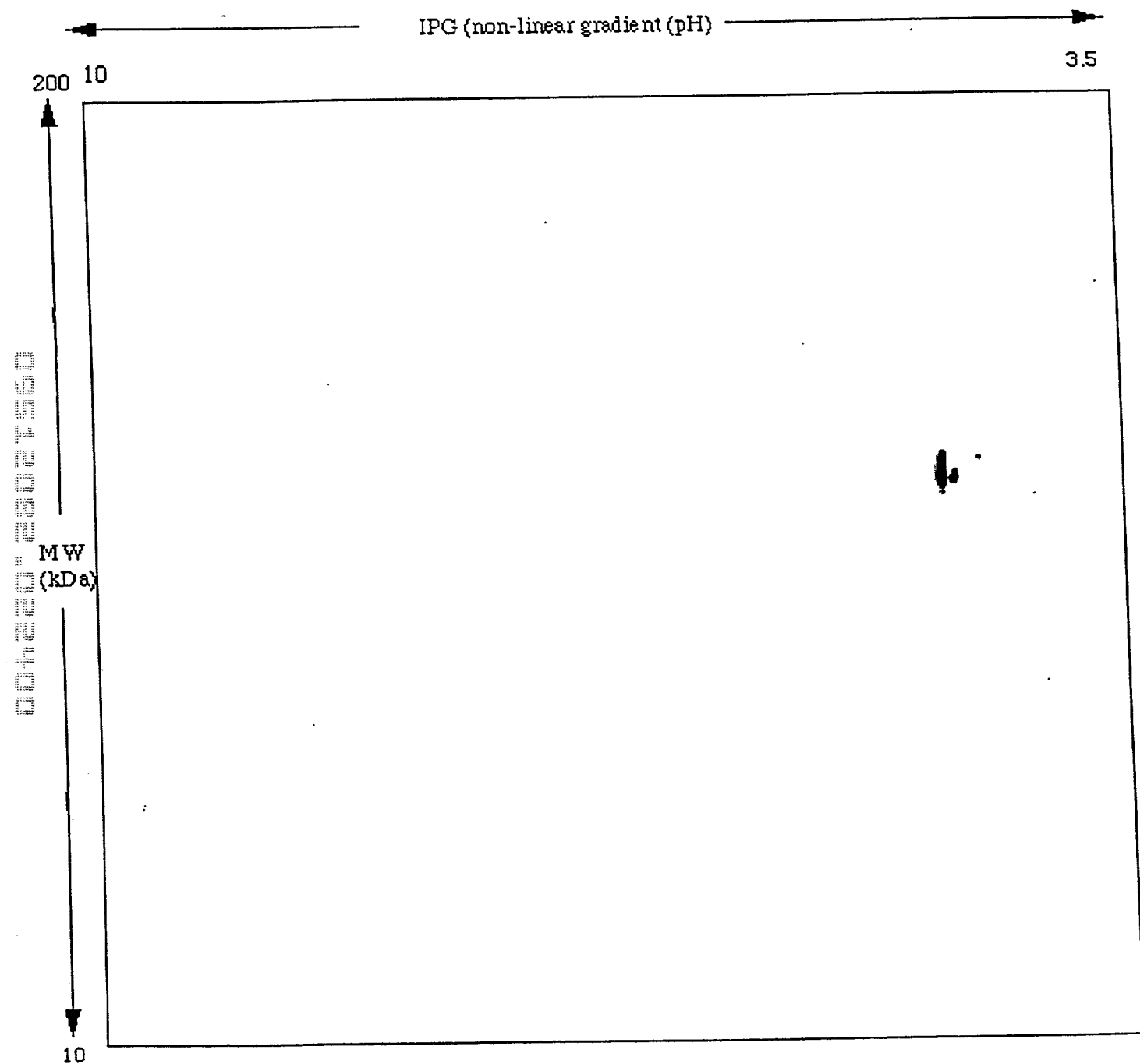


Figure 2B



Figure 3

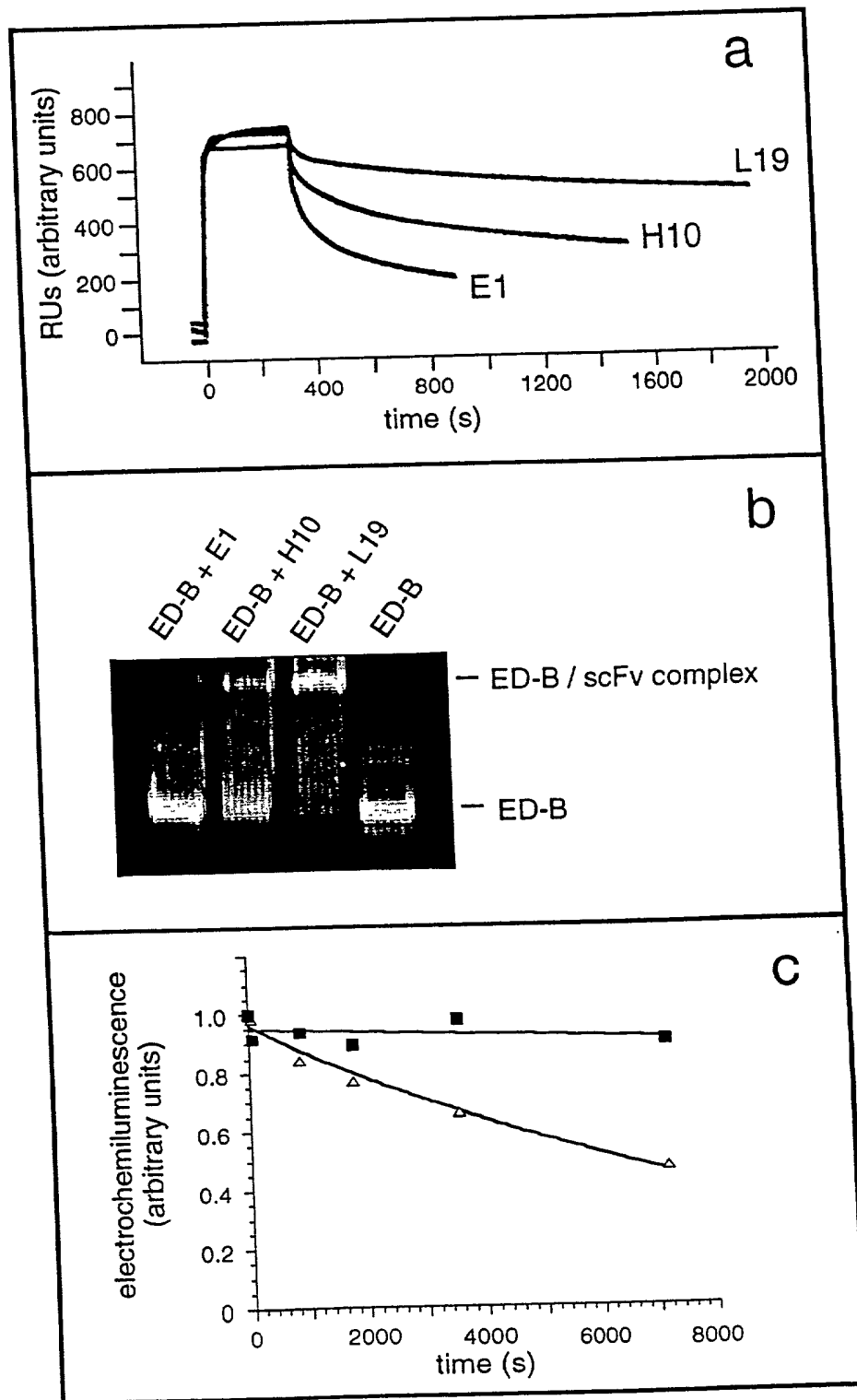
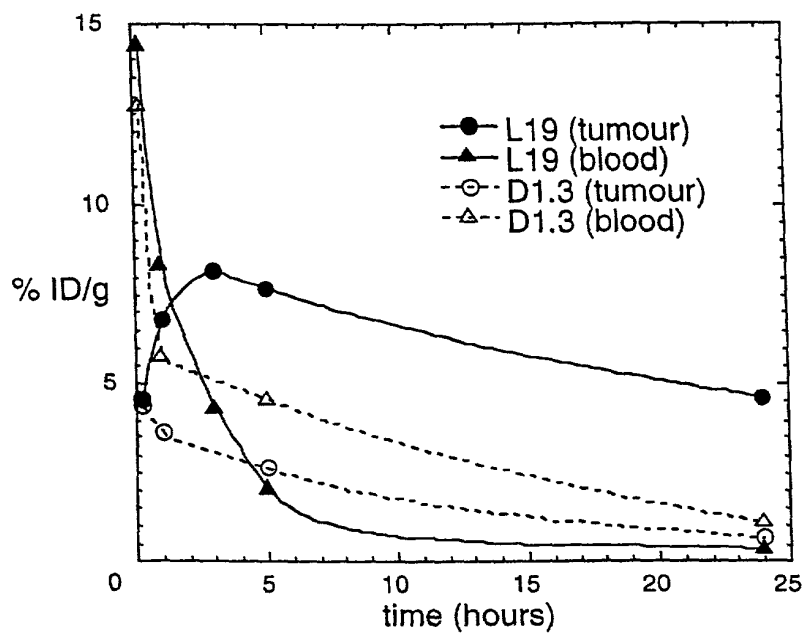


Figure 4



time (h) \ %ID/g	scFv (L19)							scFv (D1.3)	
	Kidney	Spleen	Lung	Liver	Brain	Blood	Tumor	Blood	Tumor
0.25	26.4 ± 4.7	5.4 ± 0.4	15.1 ± 5.1	5.7 ± 0.6	0.4 ± 0.04	14.4 ± 2.6	4.6 ± 1.0	12.7 ± 0.1	4.4 ± 0.4
1	19.2 ± 3.9	3.8 ± 0.3	9.8 ± 0.9	2.8 ± 0.3	0.3 ± 0.1	8.3 ± 0.9	6.9 ± 2.4	5.7 ± 0.7	3.6 ± 1.0
3	8.1 ± 1.6	2.0 ± 0.3	5.0 ± 1.4	1.7 ± 0.02	0.2 ± 0.01	4.3 ± 0.3	8.2 ± 4.2	---	---
5	4.2 ± 1.1	1.8 ± 0.2	3.5 ± 0.2	1.3 ± 0.3	0.1 ± 0.02	2.0 ± 1.6	7.7 ± 2.5	4.6 ± 1.2	2.6 ± 1.5
24	0.7 ± 0.1	0.4 ± 0.1	1.0 ± 0.1	0.2 ± 0.04	0.02 ± 0.01	0.4 ± 0.1	4.7 ± 0.6	1.1 ± 0.5	0.7 ± 0.4

Figure 5



VH

E V Q L L E S G G G	L V Q P G G S L R L	S C A A S G F T F S
S F S M S W V R Q A	P G K G L E W V S S	I S G S S G T T Y Y
A D S V K G R F T I	S R D N S K N T L Y	L Q M N S L R A E D
T A V Y Y C A K P F	P Y F D Y W G Q G T	L V T V S S

linker

G D G S S G G S G G A S T G

VL

E I V L T Q S P G T	L S L S P G E R A T	L S C R A S Q S V S
S S Y L A W Y Q Q K	P G Q A P R L L I Y	Y A S S R A T G I P
D R F S G S G S G T	D F T L T I S R L E	P E D F A V Y Y C Q
Q T G R I P P T F G	Q G T K V E I K	

Figure 6: Amino acid sequence of antibody L19



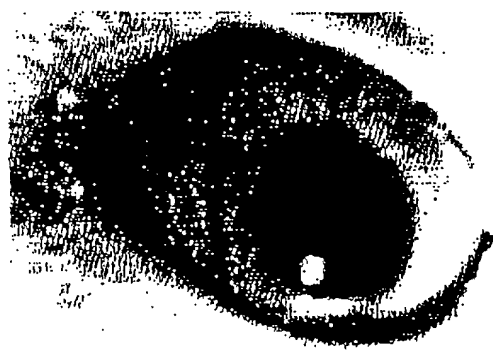
day 9 / rabbit 1 / left / nC



day 9 / rabbit 1 / right / VEGF high



day 9 / rabbit 2 / left / PMA



day 9 / rabbit 2 / left / VEGF low



day 9 / rabbit 3 / left / VEGF high



day 9 / rabbit 3 / right / PMA



day 9 / rabbit 4 / left / PMA



day 9 / rabbit 4 / right / nC

Figure 7

00420 00001560



Figure 8

FIG. 9

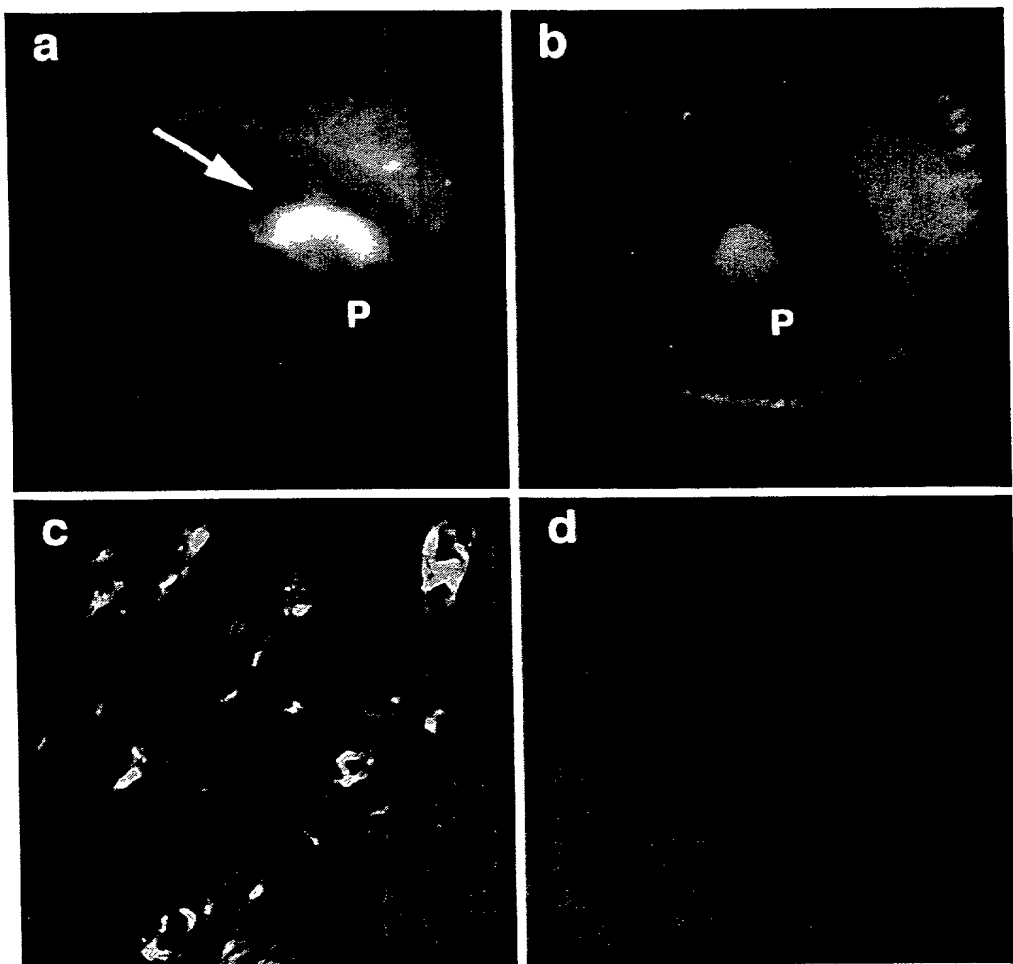


FIG. 10

Figure 1 consists of 12 black and white photographs arranged in a 4x3 grid, labeled (a) through (l). The images show the progression of a surgical procedure on a rat's head. Panels (a), (c), (e), (g), (i), and (k) show the dorsal view of the head, while panels (b), (d), (f), (h), (j), and (l) show the ventral view. Arrows and arrowheads indicate specific anatomical features and surgical steps.

FIG. 11

FIG. 12

FIGURE 13

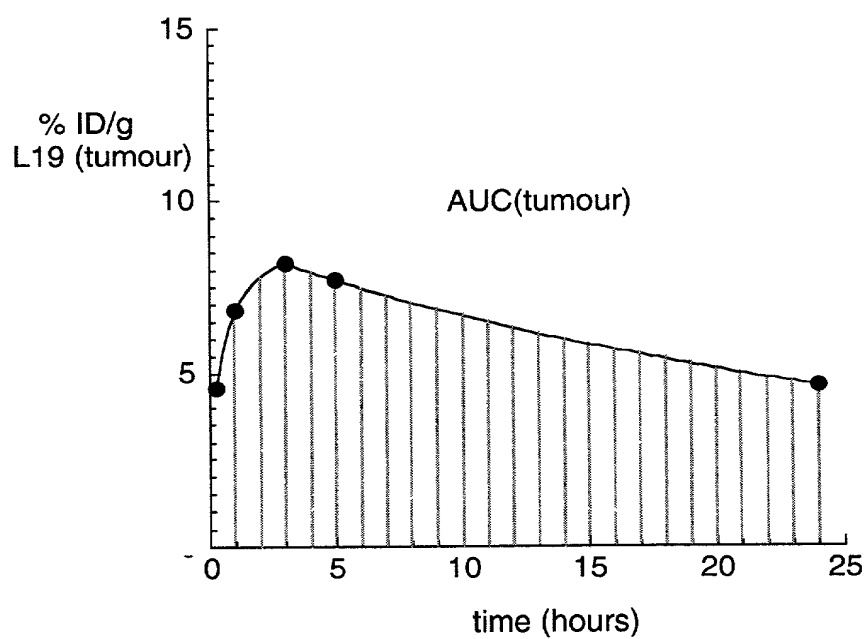
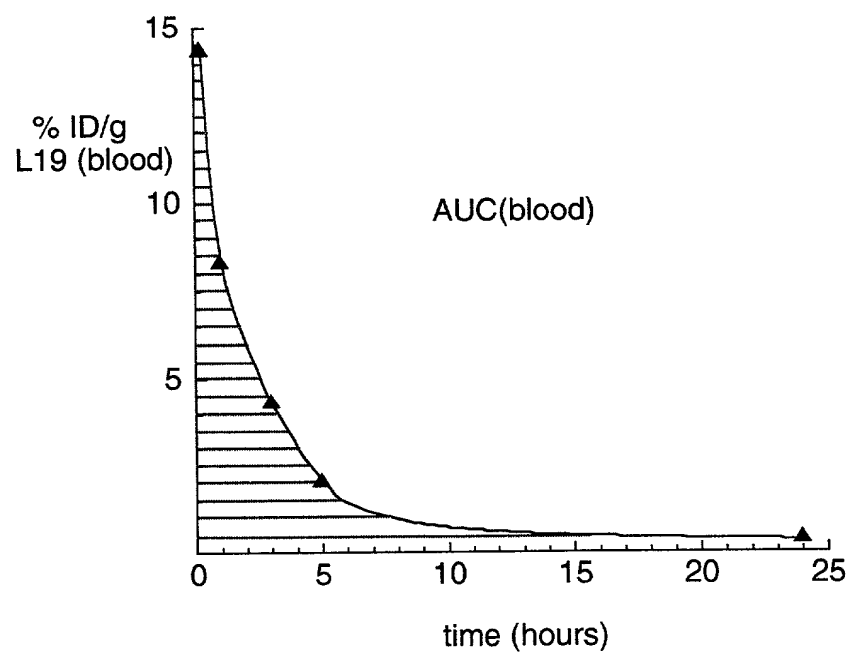




FIGURE 14

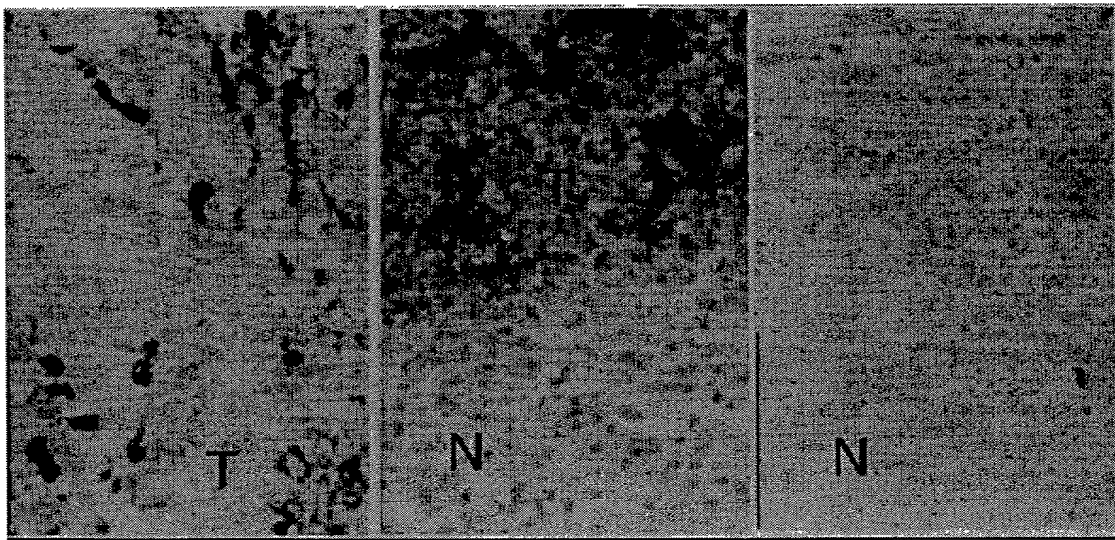
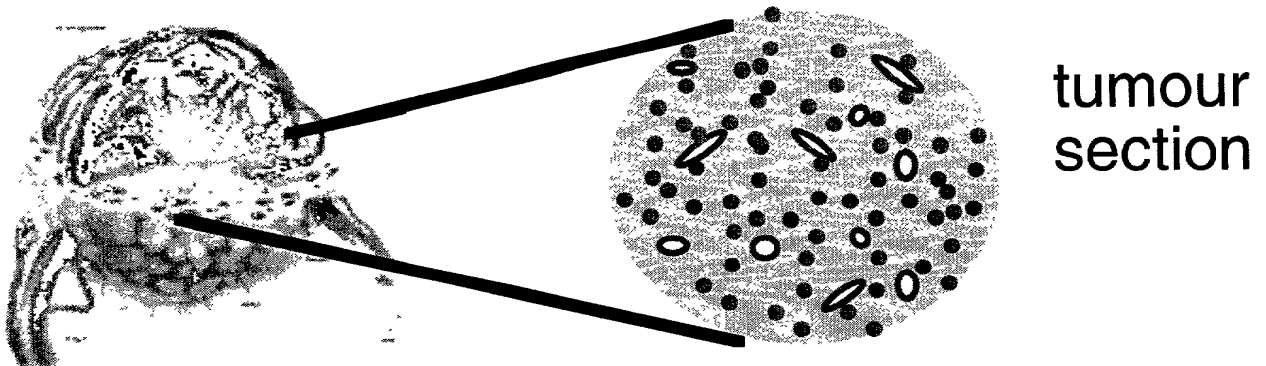


FIGURE 15

# Radioimmunotherapy with anti-angiogenesis antibodies



vessels = 0.5 - 5%  
of total tumour mass

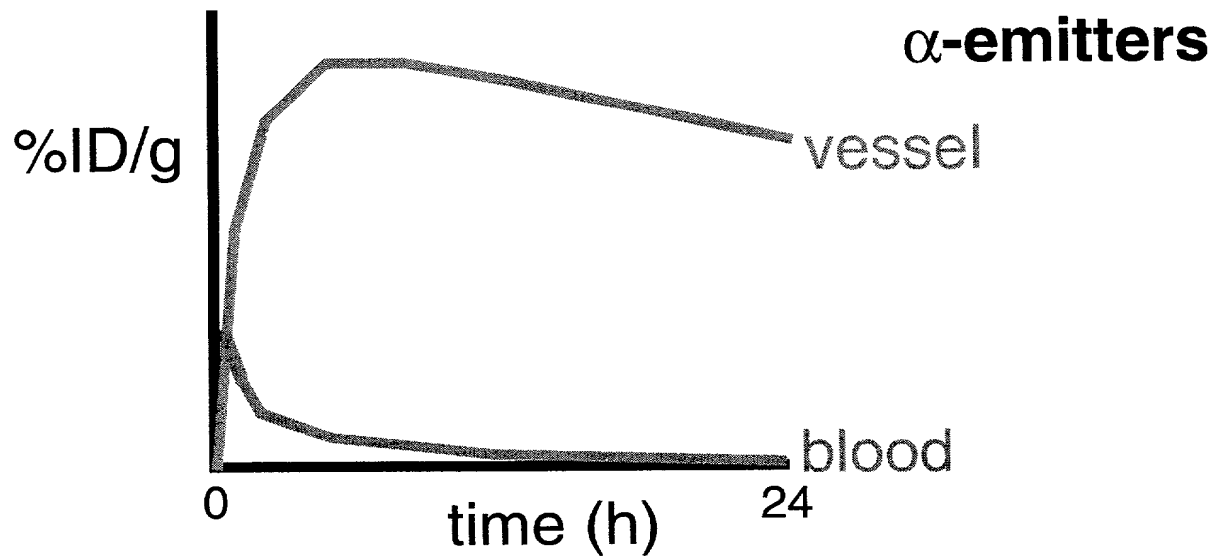
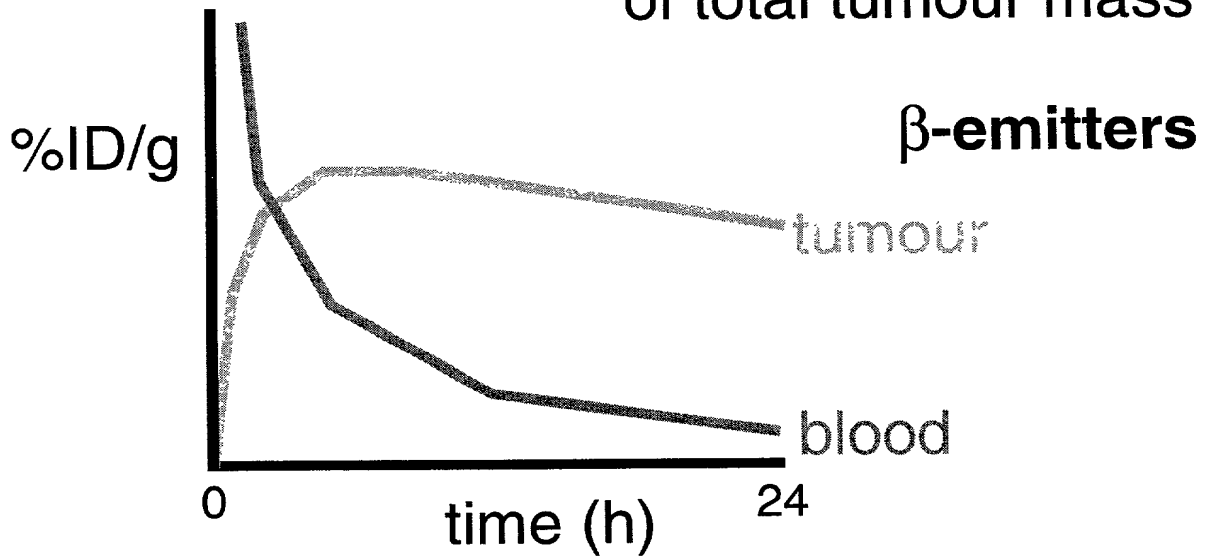


FIGURE 16

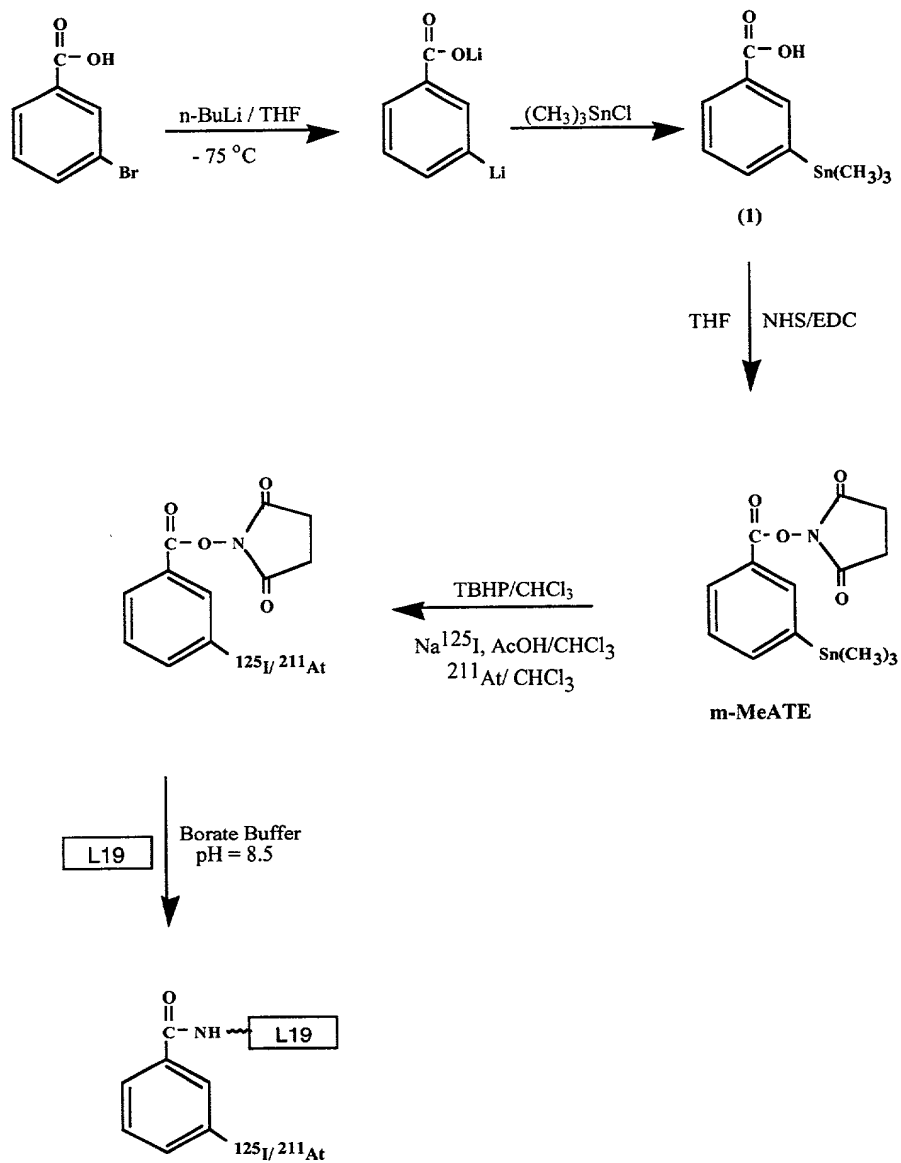
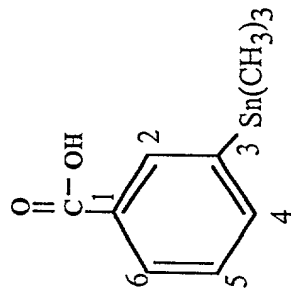


FIGURE 17a

$^1\text{H}$ -NMR spectrum of 3-(trimethylstannyl)-benzoic acid in  $\text{CDCl}_3$



$(\text{CH}_3)_3$

```

Current Data Parameters
NAME      test_0804
EXPNO     1
PROCNO    1

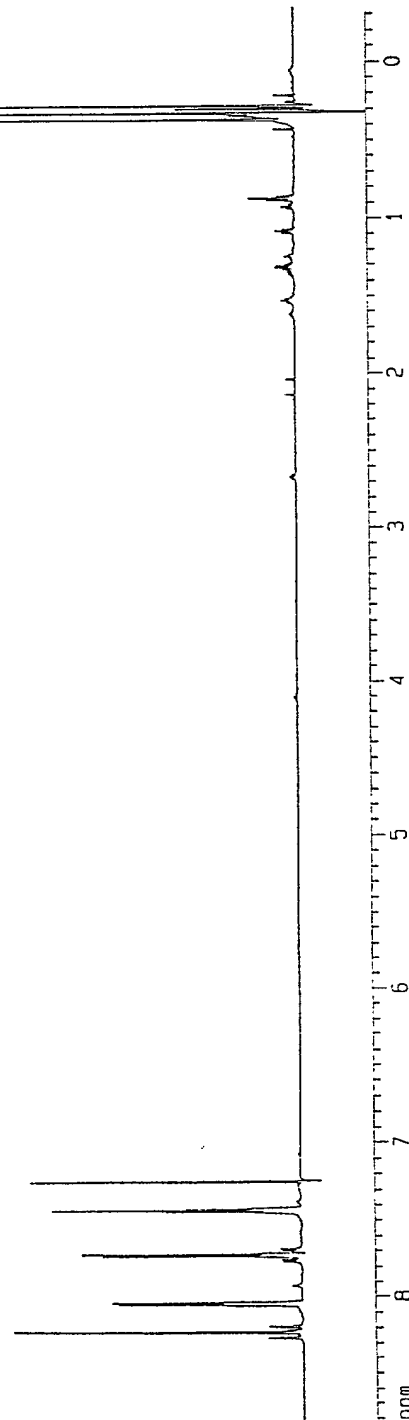
F2 - Acquisition Parameters
Date_     990804
Time      11.19
INSTRUM   drx600
PROBHD    5 mm TXI 13C
PULPROG   zgpg. eth
TD        8192
SOLVENT   CDCl3
NS        16
DS        2
SWH        9615.385 Hz
FIDRES     1.173753 Hz
AQ         0.4260340 sec
RG         800
DM         52.000 usec
DE         8.00 usec
TE         294.0 K
D1         1.00000000 sec

===== CHANNEL f1 =====
NUC1       1H
P1         8.00 usec
PL1        0.00 dB
PL9        120.00 dB
SF01       600.1328114 MHz

===== GRADIENT CHANNEL =====
GPNAM1     sine.32
GPX1       0.00 %
GPY1       0.00 %
GPZ1       50.00 %
PZ1        1000.00 usec

F2 - Processing parameters
SI         4096
SF         600.1300239 MHz
WDW        USINE
SSB        3
LB         0.00 Hz
GB         0
PC         1.00

1D NMR plot parameters
CX         20.00 cm
F1P        8.811 ppm
F1         5287.97 Hz
F2P        -0.341 ppm
F2         -204.86 Hz
PPHMC      0.45764 ppm/cm
H1C/M      274.64160 Hz/cm
    
```



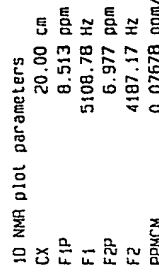
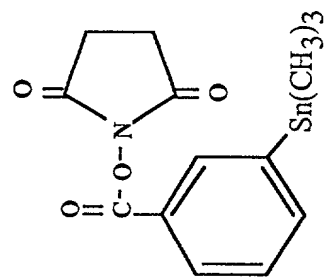
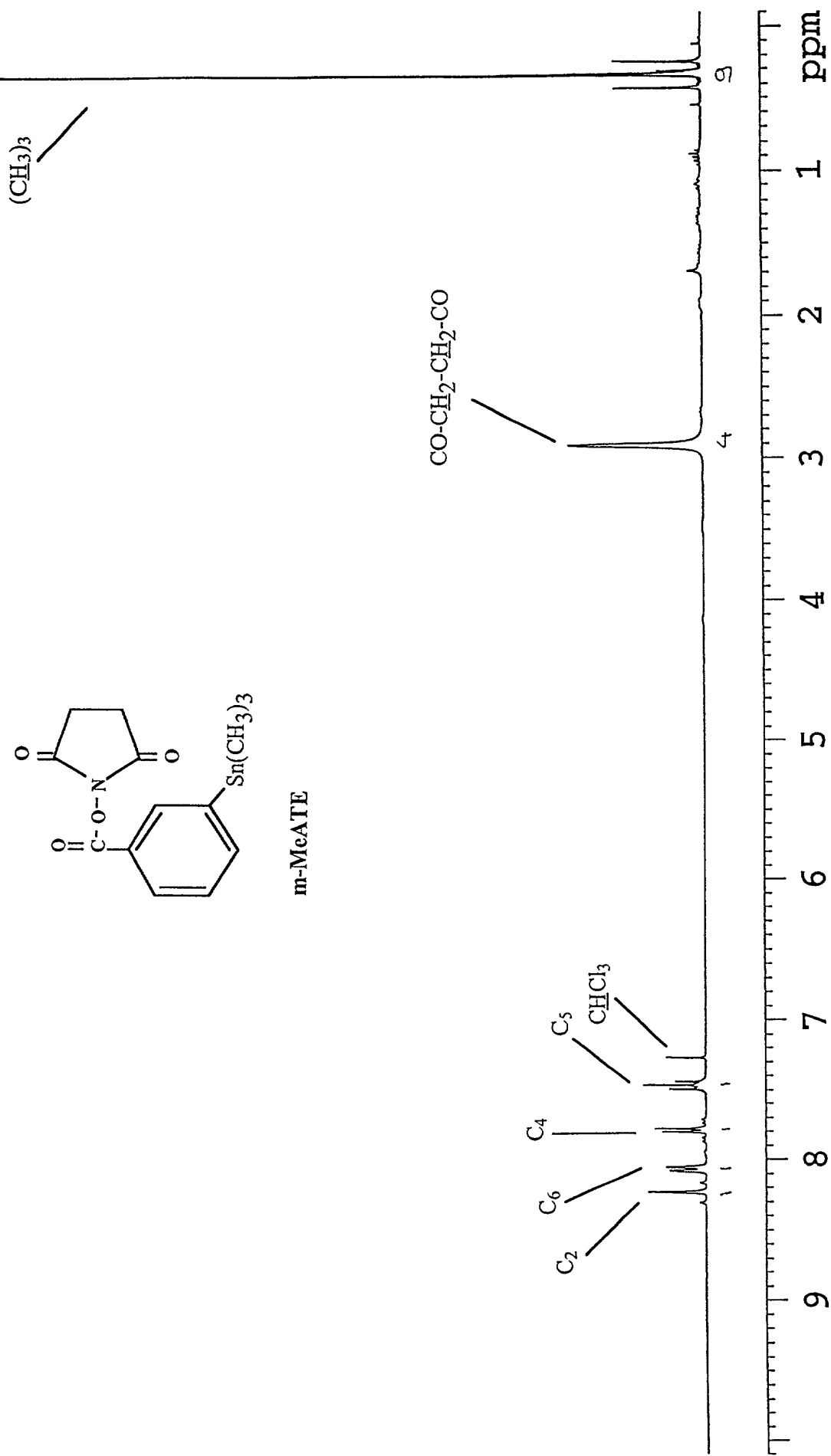
<sup>1</sup>H-NMR spectrum of 3-(trimethylstannyl)-benzoic acid in CDCl<sub>3</sub>

FIGURE 18a

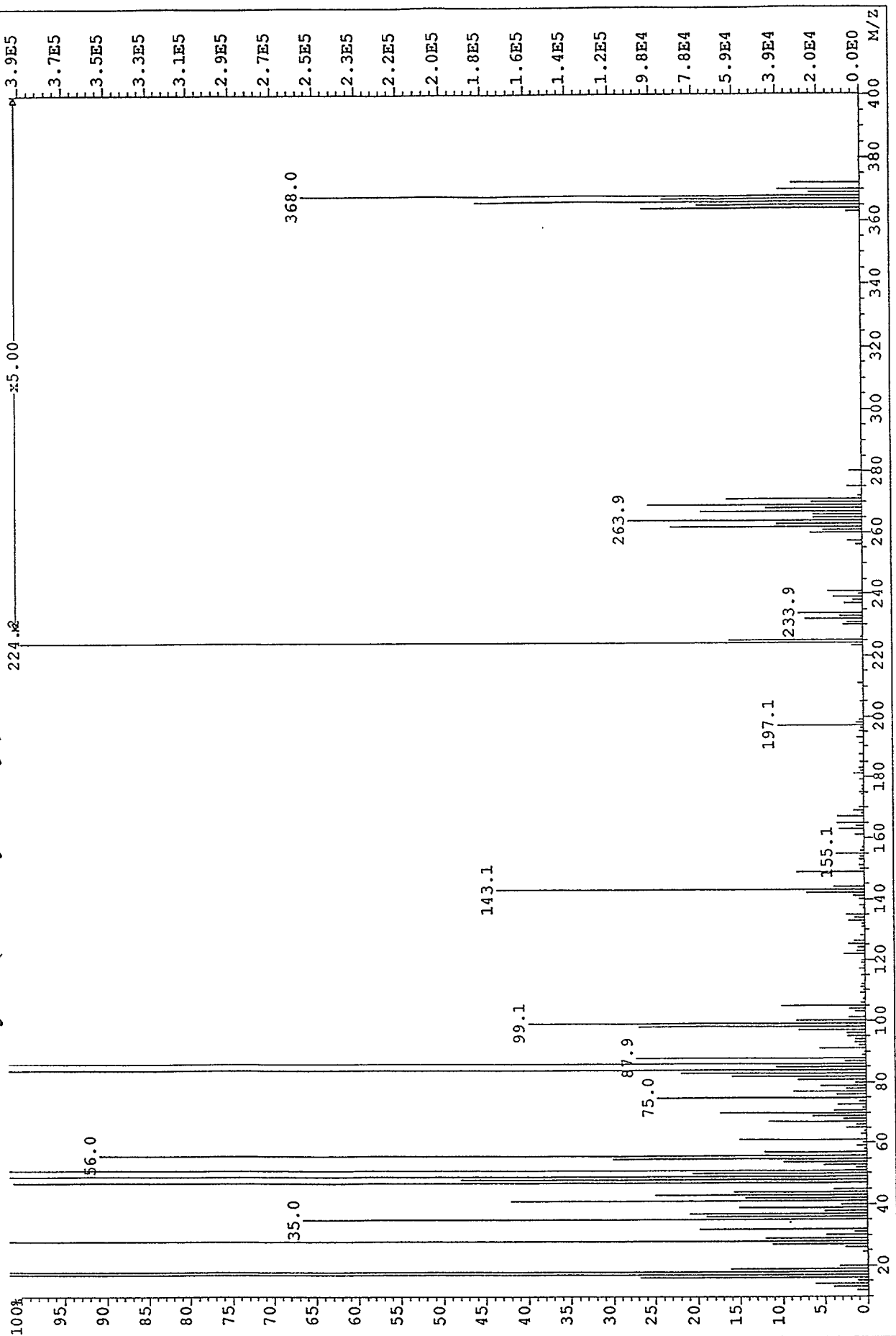
$^1\text{H}$ -NMR spectrum of N-succinimidy-3-(trimethylstannyl)-benzoate in  $\text{CDCl}_3$



m-MeATE









DECLARATION  
AND POWER OF ATTORNEY  
(Sole or Joint)

ATTORNEY'S DOCKET NO. \_\_\_\_\_

As a below named inventor, I declare that I believe I am the original, first and sole inventor if only one name is listed at Item 201 below, or a joint inventor if plural names are listed below, of the subject matter which is claimed and for which a patent is sought on the invention entitled SPECIFIC BINDING MOLECULES FOR SCINTIGRAPHY, CONJUGATES CONTAINING THEM AND THERAPEUTIC METHOD FOR TREATMENT OF ANGIOGENESIS which is described and claimed in:

☒ the attached specification ☐ the specification in application Serial No. \_\_\_\_\_, filed \_\_\_\_\_  
(for declaration not accompanying application papers)

I have reviewed and understand the contents of the above-identified specification, including the claims, as amended by any amendment referred to above.

I acknowledge the duty to disclose information of which I am aware which is material to the patentability of this application in accordance with Title 37, Code of Federal Regulations, §1.56(a).

I hereby claim the benefit of priority, under Title 35, United States Code, §119, of any foreign application(s) for patent or inventor's certificate listed below and have also identified below any foreign application(s) for patent or inventor's certificate having a filing date before that of the application for which priority is claimed.

I hereby claim the benefit, under Title 35, United States Code, §120, of any U.S. application(s) listed below. If this application is a continuation in part, insofar as the subject matter of any of the claims thereof is not disclosed in the prior U.S. application(s) identified below in the manner provided by the first paragraph of Title 35, United States Code, §112, I acknowledge the duty to disclose material information as defined in Title 37, Code of Federal Regulations, §1.56(a) which occurred between the filing date of the prior U.S. application(s) identified in Item 105 below and the national or PCT international filing date of this application.

FOREIGN APPLICATION(S), IF ANY, FILED WITHIN 12 (6 if a Design) MONTHS PRIOR TO THE FILING DATE OF THIS			
COUNTRY	APPLICATION NUMBER	DATE OF FILING (day, month, year)	PRIORITY CLAIMED UNDER 35 U.S.C. 119
U.S.A.	09/075,338	11th May 1998	YES <input checked="" type="checkbox"/> NO <input type="checkbox"/>
U.S.A.	09/300,425	28th April 1999	YES <input checked="" type="checkbox"/> NO <input type="checkbox"/>
ALL FOREIGN APPLICATIONS, IF ANY, FILED MORE THAN 12 (6 if a Design) MONTHS PRIOR TO THE FILING DATE OF THIS APPLICATION			

POWER OF ATTORNEY: As a named inventor, I hereby appoint the following attorney(s) to prosecute this application and transact all business in the Patent and Trademark Office connected therewith.

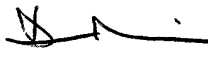
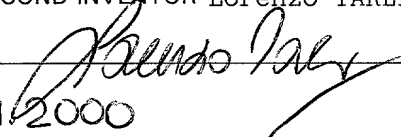
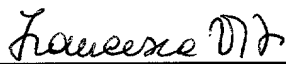
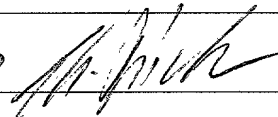
I. William Millen (19,544); John L. White (17,746); Antony J. Zelano (27,969); Alan E.J. Branigan (20,565); John R. Moses (24,983); Harry B. Shubin (32,004); Brion P. Heaney (32,542); Richard J. Traverso (30,595); John A. Sopp (33,103); Richard M. Lebovitz (37,067); John H. Thomas (33,460); Cathrine Joyce (40,668); Nancy Axelrod (P-44,104) and Jay T. Moore (35,619)

SEND CORRESPONDENCE TO: MILLEN, WHITE, ZELANO & BRANIGAN P.C. Arlington Courthouse Plaza 1, Suite 1400 220 Clarendon Blvd. ARLINGTON, VA 22201	Telephone (703) 243 6333  Telefax (703) 243 6410
--	--

Inventor(s) name must include at least one unabbreviated first or middle name.

FULL NAME OF INVENTOR	LAST NAME NERI	FIRST NAME Dario	MIDDLE NAME
RESIDENCE & CITIZENSHIP	CITY OR OTHER LOCATION Zürich	STATE OR FOREIGN COUNTRY Switzerland	COUNTRY OF CITIZENSHIP Italy
POST OFFICE ADDRESS	POST OFFICE ADDRESS Imbisbühlsteig 22	CITY Zürich	STATE OR COUNTRY Switzerland
			ZIP CODE 8049
FULL NAME OF INVENTOR	LAST NAME TARLI	FIRST NAME Lorenzo	MIDDLE NAME
RESIDENCE & CITIZENSHIP	CITY OR OTHER LOCATION Monteriggioni	STATE OR FOREIGN COUNTRY Italy	COUNTRY OF CITIZENSHIP Italy
POST OFFICE ADDRESS	POST OFFICE ADDRESS Via Abbadia 20	CITY Monteriggioni	STATE OR COUNTRY Italy
			ZIP CODE 53035
FULL NAME OF INVENTOR	LAST NAME VITI	FIRST NAME Francesca	MIDDLE NAME
RESIDENCE & CITIZENSHIP	CITY OR OTHER LOCATION Genova	STATE OR FOREIGN COUNTRY Italy	COUNTRY OF CITIZENSHIP Italy
POST OFFICE ADDRESS	POST OFFICE ADDRESS Via Battaglini 16	CITY Genova	STATE OR COUNTRY Italy
			ZIP CODE 16151
FULL NAME OF INVENTOR	LAST NAME BIRCHLER	FIRST NAME Manfred	MIDDLE NAME
RESIDENCE & CITIZENSHIP	CITY OR OTHER LOCATION Zürich	STATE OR FOREIGN COUNTRY Switzerland	COUNTRY OF CITIZENSHIP Switzerland
POST OFFICE ADDRESS	POST OFFICE ADDRESS Anwandstrasse 66	CITY Zürich	STATE OR COUNTRY Switzerland
			ZIP CODE 8004

I hereby declare that all statements made herein of my own knowledge are true and that all statements made on information and belief are believed to be true; and further that these statements were made with the knowledge that willful false statements and the like so made are punishable by fine or imprisonment, or both, under section 1001 of Title 18 of the United States Code, and that such willful false statements may jeopardize the validity of the application or any patent issuing thereon.

SIGNATURE OF FIRST INVENTOR Dario NERI	SIGNATURE OF SECOND INVENTOR Lorenzo TARLI
DATE 6 JANUARY 2000 	DATE 12.01.2000 
SIGNATURE OF THIRD INVENTOR Francesca VITI	SIGNATURE OF FOURTH INVENTOR Manfred BIRCHLER
DATE 12/01/00 	DATE 6. Jan. 2000 

<110> EIDGENOESSISCHE TECHNISCHE HOCHSCHULE ZUERICH

<130> 1900PTUS/CIP2

<140>

<141>

<150> US 09/075,338

<151> 1998-05-11

<150> US 09/300,425

<151> 1999-04-28

<160> 21

&lt;170&gt; PatentIn Ver. 2.0

<210> 1

<211> 24

<212> DNA

<213> Artificial Sequence

 $\langle 220 \rangle$ 

<223> Description of Artificial Sequence: PCR primer:  
LMB1bis

<400> 1

gcggcccagc cggccatggc cgag

24

<210> 2

<211> 54

<212> DNA

<213> Artificial Sequence

 $\langle 220 \rangle$ 

<223> Description of Artificial Sequence: PCR primer:  
DP47CDR1for

<400> 2

gagcctggcg gacccagctc atmnnmnnmn ngctaaaggt gaatccagag gctg

54

<210> 3

<211> 23

<212> DNA

### <213> Artificial Sequence

 $\langle 220 \rangle$ 

<223> Description of Artificial Sequence: PCR primer:  
DP47CDR1back

<400> 3

atgagctggg tccgccaggc tcc

23

<210> 4

<211> 60

<212> DNA

```

<213> Artificial Sequence
<220>
<223> Description of Artificial Sequence: PCR primer:
        DP47CDR2for

<400> 4
gtctgcgtag tatgtggtac cmnnactacc mnnaatmnnt gagacccact ccagcccctt 60

<210> 5
<211> 24
<212> DNA
<213> Artificial Sequence
<220>
<223> Description of Artificial Sequence: PCR primer:
        DP47CDR2back

<400> 5
acatactacg cagactccgt gaag                                     24

<210> 6
<211> 53
<212> DNA
<213> Artificial Sequence
<220>
<223> Description of Artificial Sequence: PCR primer:
        JforNot

<400> 6
tcattctcga cttgcggccg ctttgatttc caccttggtc cttggccga acg      53

<210> 7
<211> 47
<212> DNA
<213> Artificial Sequence

<220>
<223> Description of Artificial Sequence: PCR primer:
        DPKCDR1for

<400> 7
gtttctgctg gtaccaggct aamngctgc tgctaacact ctgactg              47

<210> 8
<211> 23
<212> DNA
<213> Artificial Sequence

<220>
<223> Description of Artificial Sequence: PCR primer:
        DPKCDR1back

<400> 8
ttagcctggt accagcagaa acc                                       23

<210> 9
<211> 46
<212> DNA
<213> Artificial Sequence
<220>

```

<223> Description of Artificial Sequence: PCR primer:  
DPKCDR2for

<400> 9  
gccagtggcc ctgctggatg cmnnatagat gaggagcctg ggagcc 46

<210> 10

<211> 21

<212> DNA

<213> Artificial Sequence

<220>

<223> Description of Artificial Sequence: PCR primer:  
DPKCDR2back

<400> 10  
gcatccagca gggccactgg c 21

<210> 11

<211> 45

<212> DNA

<213> Artificial Sequence

<220>

<223> Description of Artificial Sequence: PCR primer:  
DP47baNco

<400> 11  
gcggccccagc atgcatggc cgaggtgcag ctgttggagt ctggg 45

<210> 12

<211> 55

<212> DNA

<213> Artificial Sequence

<220>

<223> Description of Artificial Sequence: PCR primer:  
CDR3for

<400> 12  
ggttccctgg cccagtagt caaamnnmnn mnnmnnnttc gcacagtaat atacg 55

<210> 13

<211> 24

<212> DNA

<213> Artificial Sequence

<220>

<223> Description of Artificial Sequence: PCR primer:  
VHpullth

<400> 13  
gcggcccagc atgcatggc cgag 24

<210> 14

<211> 66

<212> DNA

<213> Artificial Sequence

<220>

<223> Description of Artificial Sequence: PCR primer:  
Jassm

```

<400> 14
cccgctaccg ccactggacc catcgccact cgagacggtg accagggttc cctggcccca 60
gtagtc 66

<210> 15
<211> 62
<212> DNA
<213> Artificial Sequence

<220>
<223> Description of Artificial Sequence: PCR primer:
        DPK22assm

<400> 15
gatgggtcca gtggcggtag cgggggcgcg tcgactggcg aaattgtgtt gacgcagtct 60
cc 62

<210> 16
<211> 63
<212> DNA
<213> Artificial Sequence
<220>
<223> Description of Artificial Sequence: PCR primer:
        DPK3for

<400> 16
caccttggtc ccttggccga acgtmnnccg mnmnnaccm nncgtctgac agtaatacac 60
tgc 63

<210> 17
<211> 56
<212> DNA
<213> Artificial Sequence
<220>
<223> Description of Artificial Sequence: PCR primer:
        Jfornot

<400> 17
gagtcattct cgacttgcgg ccgctttgat ttccaccttg gtcccttggc cgaacg 56

<210> 18
<211> 24 11
<212> DNA
<213> Artificial Sequence
<220>
<223> Description of Artificial Sequence: PCR primer:
        VLpullth

<400> 18
gatgggtcca gtggcggtag cggg 24

<210> 19
<211> 116
<212> PRT
<213> VH antibody specific for ED-B domain of fibronectin

```

Pro Thr Phe Gly Gln Gly Thr Lys Val Glu Ile Lys  
100 105